Structure and Constitution of the Lower Oceanic Crust

NIKOLAS I. CHRISTENSEN

Department of Geological Sciences and Graduate Program in Geophysics
University of Washington, Seattle, Washington 98195

MATTHEW H. SALISBURY

Department of Geological Sciences, University of Washington, Seattle, Washington 98195

Any petrologic model of the lower oceanic crust must be consistent with three sets of data: (1) the seismic structure of the oceanic crust, (2) the petrology of oceanic dredge samples, and (3) laboratory measurements of seismic velocity through such samples. A review of these data indicates that within the framework of earlier three-layer models of oceanic seismic structure the crust is internally complex and varies markedly with age, azimuth, and tectonic province. Mantle compressional wave velocities V_p are anomalously low under the ridge (7.2–7.7 km/s) but increase to 8.0–8.3 km/s beyond 15 m.y.; layer 3 thickens by 2 km within 40 m.y. of formation and decreases in V_p from 6.8 to 6.5 km/s within 80 m.y.; both the mantle and layer 3 are statistically anisotropic. Dredge lithologies consist predominantly of serpentinized ultramafics and mafic igneous rocks ranging from basalt to gabbro, the gabbro often showing evidence of fractionation. Metamorphism of mafic rocks from zeolite to amphibolite facies grade is common. Velocities in oceanic serpentinites and basalts are generally lower than layer 3 refraction velocities. Unaltered gabbros have compressional wave velocities of approximately 7.0 km/s, which is high for layer 3, together with shear wave velocities V_s of 3.8 km/s and values of Poisson's ratio σ of 0.30. Metabasites containing hornblende and plagioclase have values of V_p = 6.8 km/s, V_s = 3.8 km/s, and σ = 0.28, in good agreement with those of layer 3. On the basis of petrology and velocity it is suggested that layer 3 is composed of hornblende metagabbro underlain by normal gabbro. In a model consistent with geophysical observations of heat flow, seismicity, gravity, and seismic structure at the ridge it is proposed that layer 2 and the upper levels of layer 3 form near the median valley but that deeper levels of layer 3 thicken for 40 m.y. by intermittent offridge intrusion fed from the underlying anomalous mantle. Ophiolites in such a model represent segments of thin immature ridge crest obducted onto continental margins during subduction of a spreading ridge.

CONTENTS

INTRODUCTION

The concepts of sea floor spreading and plate tectonics have provided a framework within which significant advances have been made in understanding the tectonic evolution of the ocean basins and continents. Serious deficiencies remain, however, in our understanding of the geological processes that create new oceanic crust at the ridge crests. One reason is that although the oceanic crust and upper mantle have been defined structurally through seismic studies, little is known about their mineralogic constitution. Only when sufficiently detailed information on the distribution of rock types with depth, as well as on possible lateral variations of mineralogy within the crust and upper mantle, is obtained will an understanding of the geologic processes that form the oceanic crust be possible.

Through the success of the Deep-Sea Drilling Project (DSDP), samples representative of the entire sediment column have been recovered from more than 200 ocean basin sites. Although basalts have been recovered from the underlying basement at many of these sites, only the uppermost few percent of the oceanic crust below the sediment column have been directly sampled by drilling. The rest of the column is known only from dredge samples and from geophysics. Models of oceanic crustal structure are thus based on and expressed largely in terms of seismology, important constraints being provided by dredge sample petrology, gravity, heat flow, and magnetic data. Not surprisingly, interpretations of these data have resulted in several speculative petrologic models of the oceanic crust that differ significantly from one another.

This paper distinguishes which of these petrologic models are plausible and which are improbable through a comparison of the seismic velocity structure of the oceanic crust with velocities measured in the laboratory from samples recovered from the ocean basins. To this end, three sets of primary data are examined: (1) oceanic refraction data in the form of a new compilation of data published or summarized since 1964, (2) petrologic descriptions of oceanic dredge samples, and (3) laboratory velocity measurements of oceanic rocks, many presented here for the first time. No model presented in the literature to date appears to be entirely consistent with the constraints imposed by these data. A petrologic model of the oceanic crust satisfying these constraints is suggested. In addition, a mechanism is proposed by which such crust might be generated at the ridge crest.

SEISMIC STRUCTURE

Field Techniques

The last two decades have witnessed a remarkable increase in our knowledge of the structure of the oceanic crust, an increase due largely to seismic refraction studies at sea. The bulk of the data available from these studies has been acquired by

using the unreversed, split, and reversed techniques developed by *Ewing et al.* [1937, 1939] and more recently described by *Hill* [1952], *Shor* [1963], and *Officer et al.* [1959].

One of the more persistent problems in marine refraction studies over this period has been the proper selection of shot spacing; for operational reasons it has often been difficult to provide spacing close enough to detect layers that appear only as first arrivals over a limited shooting interval. A very promising technique introduced by *Sutton et al.* [1969], *Maynard et al.* [1969], and *Ewing and Houtz* [1969] appears to resolve this problem by producing a marked decrease in shot spacing through the use of repetitive air gun sound sources, sonobuoys, and precision echo-recording equipment. The structural resolution introduced by this technique (several previously unsuspected layers are now often detected) promises a revolution in marine refraction studies.

In increasing recognition of the complexity of the oceanic crust and upper mantle, important new shooting techniques have been developed for the study of specific problems of seismic structure. For example, following the suggestion of *Hess* [1964*a*] that seismic anisotropy may exist in the upper mantle, *Raitt et al.* [1971], *Keen and Barrett* [1971], and *Whitmarsh* [1971] have conducted orthogonal and ring surveys at sea. In perhaps the most recent instrumental development *Hussong et al.* [1969], *Francis and Porter* [1973], *Carmichael et al.* [1973], and *Lister and Lewis* [1974] have begun testing both recoverable and nonrecoverable ocean bottom seismometers used in conjunction with both conventional and air gun sources. The unique capability of these instruments to monitor both compressional and shear waves directly may be crucial to the interpretation of oceanic seismic structure in terms of petrology.

Interpretation of oceanic refraction data is relatively straightforward, and the results are generally uncomplicated. It must be emphasized, however, that such complications as velocity gradients and inversions, generally not incorporated in determinations of seismic structure, have been detected by means of amplitude and wave form analysis [*Helmberger*, 1968; *Helmberger and Morris*, 1969, 1970]. Where such compilations are present but unresolved, determinations of seismic structure, particularly layer thicknesses, may be significantly in error. Evaluation of the importance of these effects and of the validity of refraction determinations of seismic structure must await the results of additional sonobuoy and ocean bottom seismometer studies, the general application of sophisticated data analysis techniques, and, ultimately, deep basement drilling.

Oceanic Refraction Data

Compilations. More than 2000 ocean basin refraction lines have been published since the late 1930's. Since the reservations outlined above do not imply that velocities obtained from these studies are incorrect but that, at worst, they are merely incomplete, there is considerable value in compiling these data for review and interpretation. For excellent compilations of this sort the reader is referred to the works of *McConnell et al.* [1966] and *Shor et al.* [1971*a*].

Since much of the refraction data gathered by means of new techniques, as well as a large body of newly available information from back arc basins, has not been included in these compilations, it has been necessary, for the purposes of this study, to assemble a new compilation of recent refraction results. To this end, refraction velocities, layer thicknesses, and standard deviations of the data, together with water depths, profile geodetic end points and azimuths, instrumental techniques, and shooting procedures, have been compiled for 529 ocean basin sites published since 1964. In addition, an attempt has been made to assign a sea floor age to each site on the basis of magnetic anomalies and deep-sea drilling results, to classify each site in terms of tectonic province (e.g., median valley, ridge flank, back arc basin), and finally, for studies of seismic anisotropy and structure, to determine the azimuth of each profile with respect to nearby fracture zones and magnetic anomaly orientations or, for back arc basins, with respect to the axial trends of nearby island arcs and behind-arc ridges. Although extensive use will be made of this compilation below, compressional wave velocity data will be presented here in summary form only, since they can, for the most part, be found elsewhere in the literature [*Le Pichon et al.*, 1965; *Francis and Shor*, 1966; *Keen and Loncarevic*, 1966; *Ludwig et al.*, 1966, 1968, 1971, 1973; *Francis and Raitt*, 1967; *Fenwick et al.*, 1968; *Furumoto et al.*, 1968, 1971; *Murauchi et al.*, 1968, 1973; *Shor et al.*, 1968, 1971*a*, *b*; *Bunce et al.*, 1969; *Den et al.*, 1969, 1971; *Ewing and Houtz*, 1969; *Helmberger and Morris*, 1969; *Matthews et al.*, 1969; *Bosshard and MacFarlane*, 1970; *Ewing et al.*, 1970, 1971; *Houtz et al.*, 1970; *Sutton et al.*, 1971; *Talwani et al.*, 1971; *Yoshii et al.*, 1973].

Remarkably few determinations of shear wave velocity from the oceanic crust have been reported owing to the inefficiency of P to S and S to P wave conversions. Measurements that have appeared in the literature from profiles in which both V_p and V_s were reversed are listed in Table 1, together with associated values of compressional wave velocity, unit thickness, and tectonic province. In addition, Poisson's ratio σ is computed from each set of velocities and presented in Table 1. This parameter is diagnostic of mineralogy [*Christensen*, 1972*a*] and is thus critical in the interpretation of refraction velocities in terms of petrology.

Velocities and layer thicknesses. Early studies by *Hill* [1957] and subsequent analysis of numerous refraction profiles by *Raitt* [1963] suggest that the average seismic structure of the oceanic crust is surprisingly uncomplicated. Raitt's synthesis of this structure (Table 2) loosely divides the oceanic crust into three successively deeper layers on the basis of seismic velocities and layer thicknesses. Layer 1 is a thin veneer, generally less than 1 km thick, of sediments ranging in velocity from 1.5 to approximately 3.5 km/s; layer 2 is a layer of intermediate and relatively well defined thickness (generally 1.0–2.5 km) but widely ranging velocity (3.5 to approximately 6.4 km/s, the most common values lying between 4.4 and 5.6 km/s); immediately overlying the mantle, layer 3 is a layer of considerable and highly variable thickness (commonly 3.4–6.3 km) but well-defined velocity (6.4–7.7 km/s, most values lying between 6.4 and 7.0 km/s).

As can be seen in Figure 1, in which the observed velocities from all 415 main basin sites from the present compilation are presented in histogram form, the velocity layering proposed by Raitt is broadly confirmed. The general validity of this subdivision is even more apparent in Figure 2*a*, in which each velocity from the main basin sites that might be characterized as tectonically 'normal' (data from such anomalous sites as fracture zones, offridge rises, plateaus, and linear island chains are purposely excluded) is plotted against its associated layer thickness. In addition, in Figure 2*b* each mantle velocity is plotted as a function of the thickness of the overlying crust. Although subdivision of the crust into more than three layers

TABLE 1. Oceanic Shear Velocity Measurements

V_p, km/s	V_s, km/s	Poisson's Ratio σ	Unit Thickness, km	Tectonic Province	Site	Reference
2.1	0.4	0.48	0.3	Abyssal plain	6-OBS 28, 30	*Sutton et al.* [1971]
2.7	0.6	0.47	0.97	Abyssal plain	6-OBS 28, 30	*Sutton et al.* [1971]
4.7	2.5	0.30	1.05	Abyssal plain	6-OBS 28, 30	*Sutton et al.* [1971]
6.02	3.50	0.25	1.25	Behind-arc basin	N24-N25	*Shor et al.* [1971*b*]
6.35	3.55	0.27	1.18	Abyssal plain	SH 31	*Helmberger and Morris* [1969]
6.54	3.88	0.21	8.83	Offridge rise	103b	*Bunce and Fahlquist* [1962]
6.60	3.68	0.28	5.72	Behind-arc basin	27	*Murauchi et al.* [1968]
6.62	3.81	0.25	5.0	Abyssal plain	5	*Ludwig et al.* [1966]
6.65	3.84	0.25	8.22	Abyssal plain	104a	*Bunce and Fahlquist* [1962]
6.65	3.88	0.24	8.37	Abyssal plain	104b	*Bunce and Fahlquist* [1962]
6.69	3.61	0.29	4.0	Abyssal plain	LSD-6, 7	*Francis and Shor* [1966]
6.72	3.79	0.27	7.94	Offridge rise	103a	*Bunce and Fahlquist* [1962]
6.74	3.55	0.31	5.50	Offridge rise	22	*Den et al.* [1971]
6.79	3.57	0.31		Ridge flank	V-10-6	*Le Pichon et al.* [1965]
6.81	3.68	0.29	4.42	Abyssal plain	21	*Den et al.* [1971]
6.82	3.81	0.27	3.96	Behind-arc basin	21	*Den et al.* [1971]
6.83	3.78	0.28	4.91	Behind-arc basin	24	*Murauchi et al.* [1968]
6.85	3.75	0.29	3.3	Abyssal plain	6-OBS 28, 30	*Sutton et al.* [1971]
6.91	3.74	0.29	8.15	Offridge rise	3	*Den et al.* [1969]
6.94	3.85	0.28	2.75	Abyssal plain	SH 31	*Helmberger and Morris* [1969]
7.09	3.61	0.32		Ridge flank	V-10-7	*Le Pichon et al.* [1965]
7.55	4.2	0.28	2.4	Abyssal plain	6-OBS 28, 30	*Sutton et al.* [1971]
7.77	4.25	0.29		Abyssal plain	LSD-6, 7	*Francis and Shor* [1966]
8.16	4.62	0.27		Back arc basin	26-56	*Officer et al.* [1959]
8.25	4.71	0.26		Abyssal plain	6-OBS 28, 30	*Sutton et al.* [1971]
8.3	4.65	0.27		Abyssal plain	6-OBS 27	*Sutton et al.* [1971]

causes dispersal in the more recent data, each of Raitt's crustal layers, as well as the mantle, can be seen to occupy a diffuse but clearly distinguishable velocity-thickness field.

As important as such crustal averages are, it is equally important to note that information can be lost in the averaging process. By way of example, if the matter of oceanic sediment thickness had been pursued no further than a compilation of its mean, its striking dependence upon sea floor age [*Ewing and Ewing*, 1967] would have remained undetected. It is thus appropriate to point out the wide ranges in velocity and thickness included even within the standard deviations describing the mean oceanic crustal layers and to inquire as to the causes of these departures from the mean.

Variations with age. Several authors have suggested that the seismic structure of the oceanic crust varies systematically with age. The most pronounced of these variations, and the least contested, is a marked increase in the thickness of layer 3 and the total thickness of the crust with age [*Le Pichon et al.*, 1965; *Le Pichon*, 1969; *Goslin et al.*, 1972]; it has further been suggested that layer 2 thins somewhat with age [*Le Pichon*, 1969] and decreases in velocity [*Christensen and Salisbury*, 1972, 1973; *Hart*, 1973].

To examine these questions and to determine the cause of the wide ranges of thickness and velocity observed for the oceanic crustal layers, main basin refraction velocities and layer thicknesses from normal oceanic sites that can be dated are examined as a function of age (Figures 3 and 4). Since it is difficult to assign the numerous observed refraction velocities falling outside the layer-defining standard deviations to a particular layer and since it is equally difficult, for those cases in which subdivisions of a given layer are observed, to decide which velocity is characteristic of a layer, the noncommital approach of plotting velocities in histograms appropriate to their ages has been taken in Figure 3. Changes in velocity with age will thus be seen in this figure as differences in form between

TABLE 2. Average Oceanic Crustal Structure [after *Raitt*, 1963]

	Velocity V_p, km/s	Thickness, km
Layer		
2	5.07 ± 0.63	1.71 ± 0.75
3	6.69 ± 0.26	4.86 ± 1.42
Mantle	8.13 ± 0.24	

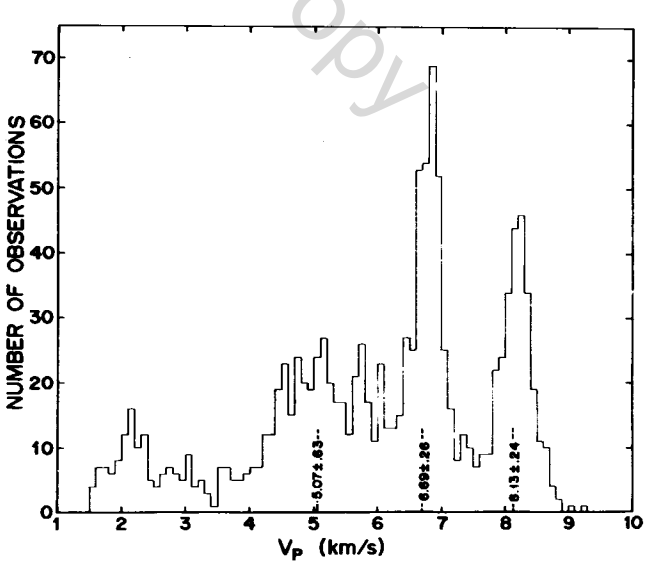

Fig. 1. Histogram of compressional wave refraction velocities from 415 main ocean basin sites. Superimposed are mean compressional wave velocities and standard deviations of velocity for layers 2, 3, and the mantle as computed by *Raitt* [1963].

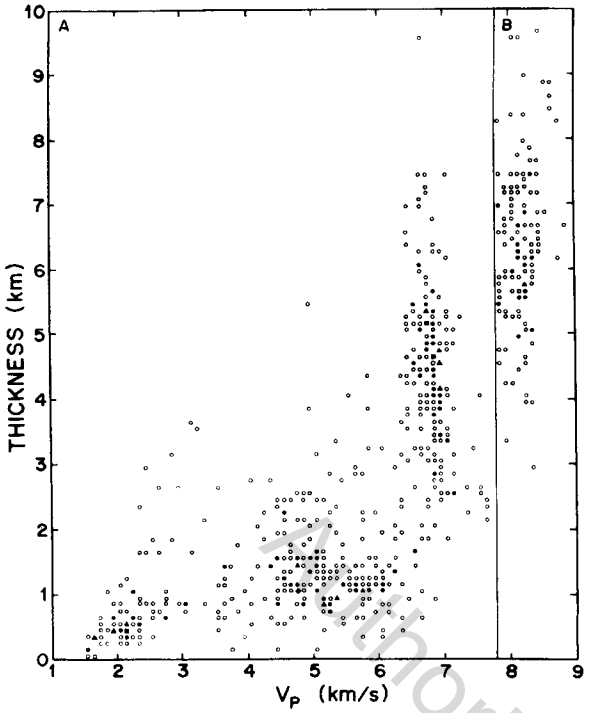

Fig. 2. (*a*) Compressional wave refraction velocities versus associated layer thicknesses from normal main ocean basin sites. (*b*) Mantle compressional wave velocity versus cumulative thickness of overlying crustal layers. Open circles indicate 1 observation; solid circles, 2 observations; solid triangles, 3 observations; solid squares, 4 observations; solid diamonds, 5 observations.

histograms. Two such changes are readily apparent. (1) 'Anomalous mantle' refraction velocities ranging between 7.1 and 7.8 km/s are frequently observed in young crust but are almost absent in crust more than 40 m.y. old. When velocities of this range are present, normal mantle velocities are usually absent, and layer 3 velocities are missing or slow. It should be pointed out that the presence of this phenomenon is spotty even in young crust; an equal number of sites are found with a normal seismic structure. (2) Velocities in the range 6.7–6.9 km/s (i.e., the range of velocities commonly regarded as most characteristic of layer 3) are seen to dominate lower crustal velocities in young regions but are virtually absent in crust more than 80 m.y. old, being replaced by a bimodal distribution of velocities centering around peaks at 6.5 and 7.0 km/s. As to the suggestion that layer 2 velocities decrease with age, Figure 3 is inconclusive owing to data dispersal caused by the introduction of velocity subdivisions in layer 2 in recent data included in the figure. Histograms of layer 2 velocities from standard three-layer models of oceanic crustal structure continue to show few observations of high velocity in layer 2 in old crust, a finding consistent with a downward shift in velocities with age.

If the thicknesses of layers 2 and 3 are plotted as a function of age (Figure 4), layer 2 is seen to decrease slightly and layer 3 to increase markedly in thickness with age (from 1.8 to 1.35 km and from 3.0 to 4.8 km, respectively) to about 40 m.y., beyond which time little change is observed. Although both observations are consistent with those of *Le Pichon* [1969] and although the observation that layer 3 thickens with age is almost certainly valid, the statement that layer 2 thins with age is misleading without further clarification. The majority of the young sites examined in this figure do not display an abnormally thick layer 2. A small number of young sites, however, have layer 2 thicknesses that are two to three times normal, and, as a consequence, the average thickness is slightly greater than that of old crust. An alternative and attractive interpretation of the data is not that layer 2 is abnormally thick but that layer 3 velocities are strongly depressed at these sites, these depressions causing layer 3 to be geophysically indistinguishable from layer 2 and thus added to its base. It is notable in this connection that young sites displaying such apparent thickening also display, almost invariably, anomalous mantle velocities. It is thus felt that abnormal layer 2 thicknesses, a thin or absent layer 3, and the presence of anomalous mantle velocities are interrelated phenomena at many young sites. The plate tectonic setting of these sites, their spotty geographic distribution, and their unusual structure suggest that they may be sites of active intrusion.

Menard [1967] and *Shor et al.* [1971*a*] have suggested alternatively that variations in layer 2 thickness are associated with variations in spreading rate, layer 2 being thickest at sites of slow spreading. Although this suggestion is attractive, it is difficult to evaluate. The argument hinges on data from a small number of ridge crest sites displaying slow spreading. Since the presence of an anomalous mantle is also associated with slow spreading, neither variable can be isolated as the cause of the high values of layer 2 thickness. It should be noted, however, that if the thickness of layer 2 is controlled by spreading rate only, Figure 4 implies that spreading is slower now than at any time during the previous 150 m.y., a conclusion considered unrealistic.

If many sites on the ridge crest are anomalous, it is more appropriate to compute the structure of the 'normal oceanic crust' from those sites in Figure 4 that are more than 40 m.y. old, as is done in Table 3. The mean layer velocities and standard deviations in this table are not significantly different from those in Table 2. It is worth noting, however, that the thickness of layer 2 and the standard deviations of the thicknesses of layers 2 and 3 are less than those of previous compilations.

Anisotropy. It is well established that seismic anisotropy exists in the uppermost mantle in many, though not all, areas of the main ocean basins, velocities generally being high perpendicular to ridge crests and slow parallel to ridge crests [*Hess,*

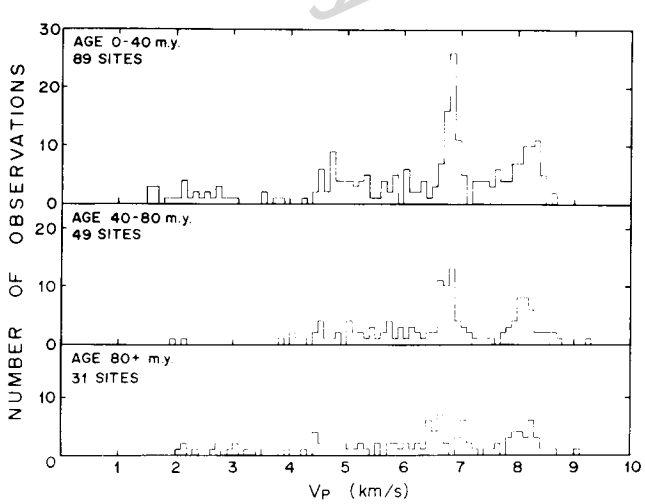

Fig. 3. Compressional wave refraction velocities from normal main ocean basin sites as a function of sea floor age.

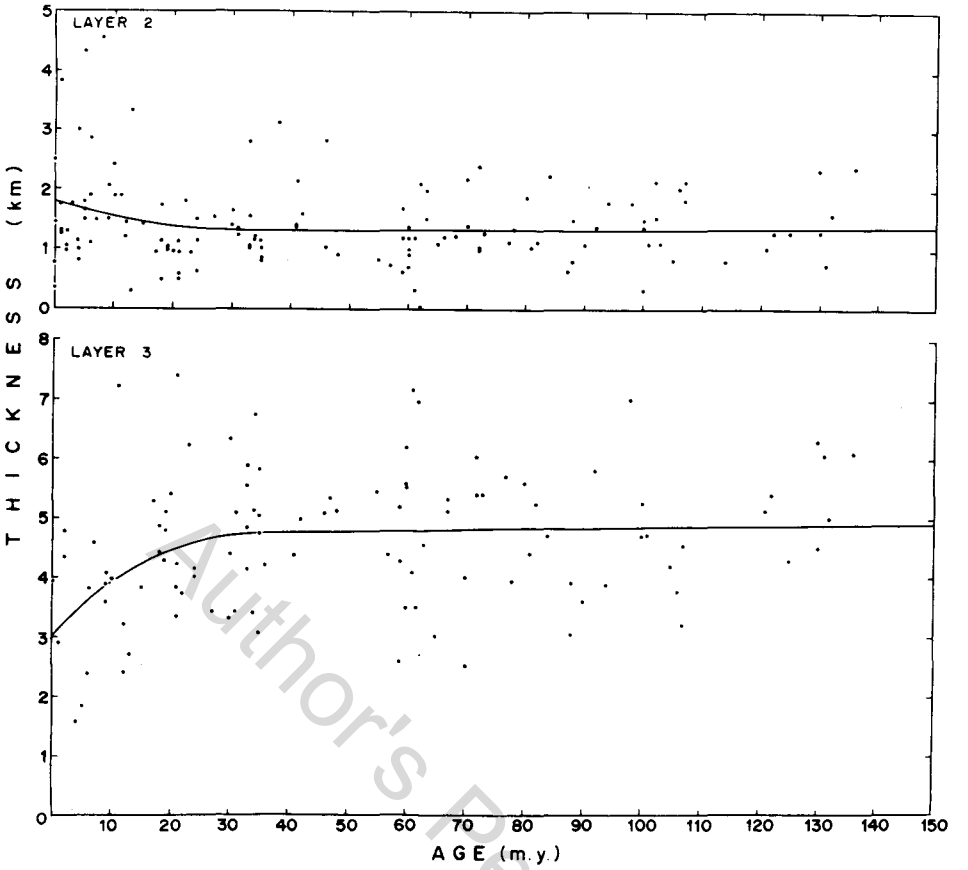

Fig. 4. Thicknesses of layers 2 and 3 at normal main ocean basin sites as a function of sea floor age. Curves are computed by running average techniques.

1964*a*; *Raitt et al.*, 1971; *Keen and Barrett*, 1971; *Whitmarsh*, 1971]. Little attention has been given, however, to whether anisotropy exists at higher levels in the oceanic crust, as was suggested by *Christensen* [1972*b*]. To resolve this question, velocities from the refraction profiles that were conducted over normal oceanic crust in the main ocean basins and that can be oriented with respect to either fracture zones or magnetic anomaly patterns (which are roughly perpendicular and parallel, respectively, to the ridge crests) are presented in histogram form in Figure 5. Profiles conducted subparallel to the ridge crests (i.e., profiles for which the difference in azimuth between the shot line and the ridge axis is <30°) are presented in the uppermost histogram, whereas those of intermediate (30°–60°) and subperpendicular (60°–90°) orientations are included in the middle and lower histograms, respectively.

The well-known anisotropy of the mantle can be clearly discerned as a marked increase in mantle velocities from a mean of 8.0 km/s subparallel to the ridge crest to a mean of 8.3 km/s subperpendicular to the ridge crest. More unexpectedly, layer 3 velocities decrease somewhat with increasing relative azimuth, a trend opposite in sense to that of the underlying mantle but consistent with recent observations by *Christensen* [1972*b*].

TABLE 3. Normal Oceanic Crustal Structure (This Study)

	Velocity V_p, km/s	Thickness, km
Layer		
2	5.04 ± 0.69	1.39 ± 0.50
3	6.73 ± 0.19	4.97 ± 1.25
Mantle	8.15 ± 0.31	

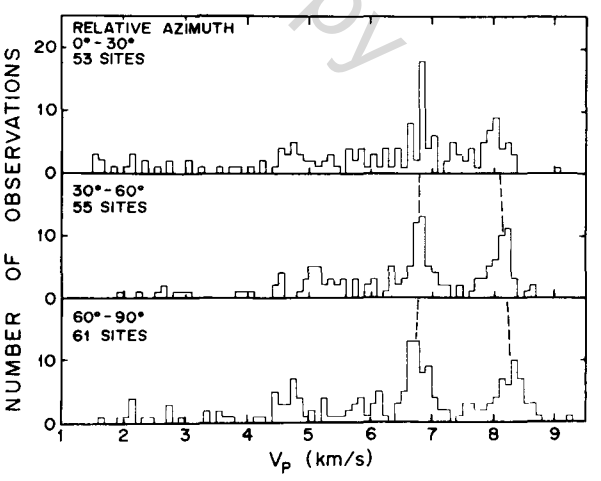

Fig. 5. Compressional wave refraction velocities from normal main ocean basin sites as a function of the azimuth of each refraction profile with respect to the local ridge axis; profiles shot subparallel to the ridge have relative azimuths of 0°–30°; those shot subperpendicular have relative azimuths of 60°–90°.

Regional variations. Despite an acknowledged genetic simplicity within the framework of plate tectonics, it is becoming increasingly clear that the oceanic crust, far from being simple, is tectonically complex. It would be remarkable if distinct features of the oceanic crust such as ridge crests, ridge flanks, abyssal plains, fracture zones, offridge rises, linear island chains, troughs and trenches, back arc basins, and rises, all clearly distinguishable in terms of topography, seismicity, and heat flow, were indistinguishable in terms of underlying seismic structure.

That major distinctions in seismic structure from province to province can be drawn has already been demonstrated (Figures 3 and 4) for the ridge crest, ridge flank, and abyssal plain provinces. Distinctions among the other provinces noted above cannot be demonstrated statistically because of insufficient data. Nonetheless, the following impressions can be noted from examination of the data. The fracture zones commonly display a conventional three-layer structure that can often be distinguished from that of normal crust in two ways. First, it is frequently thin, consistent with isostatic arguments; second, layer 2 velocities in the fracture zones are invariably low (4.2–5.4 km/s), consistent with intense brecciation. The crustal structures of offridge rises and linear island chains can commonly be distinguished from the structure of normal oceanic crust by their great thickness [*Den et al.*, 1969]. In the case of offridge rises, this increased thickness is distributed among all layers of what otherwise appears to be a conventional three-layer structure. Linear island chains, on the other hand, commonly have an unusual structure in which layer 2 is two to three times normal thickness and exhibits a wide range of velocities (3.5–6.1 km/s) distributed among several subdivisions, whereas layer 3 has somewhat low velocities and a normal thickness [*Furumoto et al.*, 1968, 1971]. Except for unusually thick sediment accumulations, the crustal structure of troughs, trenches, and back arc basins appears to be indistinguishable from that of normal oceanic crust [*Murauchi et al.*, 1968; *Ludwig et al.*, 1971]. Behind-arc rises, like main basin offridge rises, are distinguished chiefly by an unusually thick crust, the excess thickness again being distributed among layers of normal velocity [*Shor et al.*, 1971*b*].

Local structure. Recent studies using air gun–sonobuoy techniques suggest that the seismic structure of the oceanic crust may be far more complex than had previously been suspected [*Sutton et al.*, 1969; *Maynard et al.*, 1969; *Hussong*, 1972]. Although the results of routine refraction studies are generally consistent with those of sonobuoy studies [*Hussong*, 1972], the mean oceanic crustal layers of Raitt are only averages of layers that, in detail, are each seen to be composed of several subdivisions. In particular, layer 2 is frequently observed to have a thin low-velocity cap (2.5–3.8 km/s), and layer 3 is often observed to have a thick previously undetected basal layer with velocities ranging from 7.1–7.7 km/s. This layer is not to be confused with the anomalous mantle observed under ridge crests. The persistence of these subdivisions has prompted some authors [*Talwani et al.*, 1971; *Peterson et al.*, 1974] to suggest a redefinition of the mean oceanic crust based on sonobuoy data, such as the one in Table 4.

In view of the fact that only a small number of sites have been studied to date by sonobuoy techniques and that many of these show three or, in some instances, no subdivisions, such definitions seem premature. It is proposed that equally valid subdivisions of oceanic crustal structure can be drawn vertically. If the data for those main basin normal crust sonobuoy sites for which mantle returns have been observed (sufficient acoustic energy for examination of the entire column thus being insured) are plotted in a velocity-depth curve (Figure 6), two crustal types with distinctly different lower crustal (layer 3) structures are apparent. In type 1 (Figure 6) layer 3 is composed, on the average, of a 1-km-thick relatively low velocity (6.4 km/s) layer underlain by a 5-km-thick layer with a velocity of 7.1 km/s. In type 2, on the other hand, layer 3 is composed of two subdivisions, each about 3 km thick, with velocities averaging 6.8 and 7.5 km/s, respectively. Since no other criteria such as sea floor age, spreading rate, or tectonic province seem to distinguish these two crustal types (and there will almost certainly be more as more sonobuoy data become available), this variation is attributed to local structural or petrologic heterogeneity.

TABLE 4. Oceanic Crustal Structure From Sonobuoy Studies [after *Peterson et al.*, 1974]

	Velocity V_p, km/s	Thickness, km
Layer		
1	1.7–2.0	0.5
2A	2.5–3.8	0.5–1.5
2B	4.0–6.0	0.5–1.5
3A	6.5–6.8	2.0–3.0
3B	7.0–7.7	2.0–5.0
Mantle (4)	8.1	

In view of (1) the demonstrated lateral heterogeneity of the oceanic crust on both local and regional levels, (2) the impending overhaul of refraction studies and conclusions from sonobuoy data (for example, if a layer with a seismic velocity of 7.1–7.7 km/s is generally present at the base of layer 3, a slight revision of layer 3 and crustal thicknesses will be necessary), and (3) the likelihood that even this overhaul will be inaccurate owing to the presence of undetected velocity inversions and gradients, a revision of the estimates of mean oceanic crustal structure beyond that of Table 3 seems inappropriate at this time.

ROCKS FROM THE LOWER OCEANIC CRUST

The seismic structure of the oceanic crust must ultimately be interpreted in terms of petrology. It is thus important to consider what lithologies are actually recovered from the sea floor itself.

Through the efforts of deep-sea dredging and, more recently, the DSDP, igneous rocks comprising the uppermost hard-rock part of the oceanic crust have been obtained at many sites in the ocean basins. Although significant differences in chemistry exist among these rocks in restricted localities, numerous studies have shown that rocks from the uppermost basement are usually basaltic, and most have chemical characteristics that make it appropriate to call them tholeiites [*Engel and Engel*, 1964; *Engel et al.*, 1965; *Aumento*, 1967; *Miyashiro et al.*, 1969*b*; *Shido et al.*, 1971]. For more detailed information on the petrology and chemistry of submarine basalts, the reader is referred, in addition, to the excellent studies of *Aumento* [1968], *Hekinian and Aumento* [1973], and *Kay et al.* [1970].

Although several investigations [*Christensen*, 1970*a*, 1972*c*; *Christensen and Shaw*, 1970] have shown that compressional wave velocities measured in these basalts agree well with the

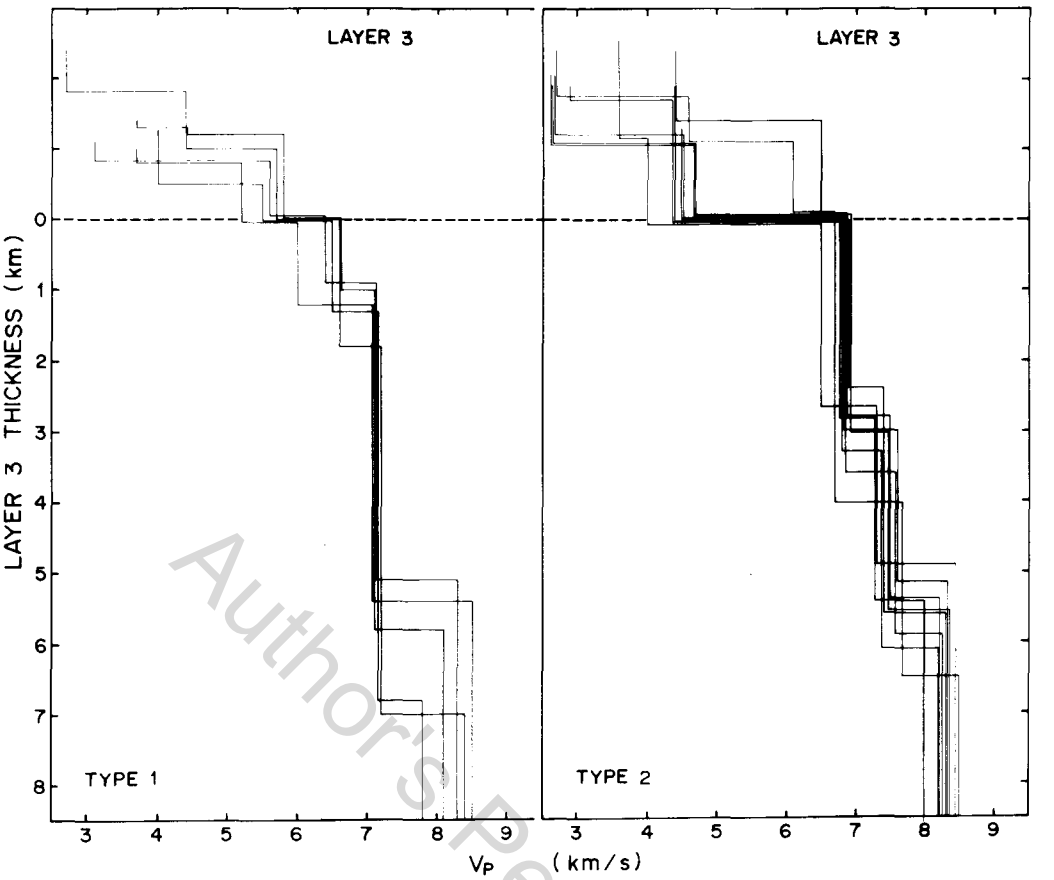

Fig. 6. Oceanic crustal types based on internal structure of layer 3 observed in sonobuoy studies conducted over normal main ocean basin sites. The range of commonly observed layer 3 refraction velocities is superimposed for comparison. Layers above the dotted line represent subdivisions of layer 2.

seismic velocities of layer 2, measured basalt velocities are generally much lower than the seismic velocities of the lower oceanic crust. For this reason we shall concentrate in the following discussion on reported occurrences and petrographic descriptions of metamorphic and coarse-grained igneous rocks dredged, for the most part, from the walls of median valleys, fracture zones, and trenches, which have been postulated to be important constituents of the lower oceanic crust. Because many of the papers that have reported the occurrences of these rocks were preliminary in nature, detailed data on the mineralogy and chemistry of possible lower crustal rocks, data that are critical in the interpretation of petrology in terms of mineralogy, are relatively limited.

Ultramafic rocks. Ultramafic rocks ranging from almost completely fresh to totally serpentinized are common constituents of fracture zones, central rift valleys, and walls of major trenches. Mineralogy indicates that the original ultramafics were dunite [*Bonatti,* 1968], lherzolite [*Engel and Fisher,* 1969; *Bonatti,* 1968; *Bonatti et al.,* 1970], harzburgite [*Cann and Funnell,* 1967; *Muir and Tilley,* 1966; *Fisher and Engel,* 1969; *Hekinian and Aumento,* 1973; *Bonatti et al.,* 1970], and picrite [*Melson and Thompson,* 1971; *Bonatti et al.,* 1970; *Ploshko and Bogdanov,* 1968]. Chemical analyses reported by *Hess* [1964*b*], *Chernysheva and Bezrukov* [1966], *Hekinian* [1968], *Bonatti* [1968], *Fisher and Engel* [1969], *Miyashiro et al.* [1969*a*], *Melson and Thompson* [1970], *Christensen* [1972*a*], and *Hekinian and Aumento* [1973] show trends related to the degree of serpentinization, sea floor weathering, and heterogeneity in the parent rocks from which the serpentinites and partially serpentinized ultramafics were formed. *Miyashiro et al.* [1969*a*] have attached particular significance to the CaO contents of oceanic serpentinites and have shown that with decreasing CaO and Al_2O_3, the K_2O and TiO_2 contents and the Fe/Mg ratio also tend to decrease. They attribute these findings to upper mantle heterogeneity and chemical migration during serpentinization.

Early studies of oceanic serpentinites [*Nicholls et al.,* 1964; *Quon and Ehlers,* 1963; *Bowin et al.,* 1966; *Hekinian,* 1968] reported antigorite as the most abundant serpentine mineral. The optical identification of antigorite has proven to be unreliable (e.g., antigorite was often equated with bastite), and more recent X ray diffraction studies have shown that lizardite is the most common serpentine mineral in oceanic ultramafics [*Miyashiro et al.,* 1969*a*; *Hekinian and Aumento,* 1973; *Aumento and Loubat,* 1971]. On the basis of oxygen and hydrogen isotopic analyses of 20 serpentinites from the mid-Atlantic ridge, the Blanco fracture zone, and the Puerto Rico trench, *Wenner and Taylor* [1973] conclude that seawater is the dominant type of water involved in the formation of oceanic serpentine from ultramafic rocks, although it is possible that up to 25% of the water involved in submarine serpentinization is magmatic in origin.

On the basis of reported occurrences, petrography, and chemistry, it is apparent that oceanic ultramafic rocks have formed under a wide variety of conditions. *Fisher and Engel* [1969] and *Melson and Thompson* [1970] have described collections of rocks from the Tonga trench and the Romanche fracture zone, respectively, that have textures and mineralogies

suggestive of layered igneous complexes. The ultramafics found within these rock suites are interpreted as representing the lower parts of crystal cumulates formed from basic magma trapped within the crust. *Bonatti* [1968] and *Bonatti et al.* [1970] have described ultramafics from the lower slopes of the Saint Paul, Romanche, and Chain fracture zones, which are overlain by a complex assemblage of metamorphics, gabbro, and basalt. *Miyashiro et al.* [1970*b*], on the basis of a dredge haul on a crestal mountain adjacent to the junction of the median valley of the mid-Atlantic ridge with the Atlantis fracture zone, have shown that ultramafics are not confined to deep levels of the oceanic crust. This finding is supported by *Thompson and Melson* [1972], who report ultramafic rocks capped by volcanics in the Vema fracture zone and suggest that the ultramafics, in this instance, represent a mantle-derived intrusion. In addition, *Aumento and Loubat* [1971] have described diapiric ultramafics at 45°N in the Atlantic that apparently are not associated with transform faults.

Gabbroic rocks. Dredge hauls have recovered a wide variety of gabbroic rocks, including two-pyroxene gabbros [*Quon and Ehlers*, 1963; *Bogdanov and Ploshko*, 1967; *Engel and Fisher*, 1969; *Bonatti et al.*, 1970; *Miyashiro et al.*, 1970*a*; *Melson and Thompson*, 1970; *Hekinian and Aumento*, 1973], norite [*Bonatti et al.*, 1970; *Bogdanov and Ploshko*, 1967], hornblende gabbro [*Cann and Vine*, 1966; *Bogdanov and Ploshko*, 1967; *Fisher and Engel*, 1969; *Bonatti et al.*, 1970; *Miyashiro et al.*, 1970*a*; *Thompson*, 1973], nepheline gabbro [*Bonatti et al.*, 1970; *Thompson and Melson*, 1972], anorthositic gabbro [*Quon and Ehlers*, 1963], anorthosite [*Engel and Fisher*, 1969], and troctolite [*Miyashiro et al.*, 1970*a*]. Petrographic descriptions and modal analyses of several of these gabbroic rocks are summarized in Table 5.

The association of gabbro, anorthosite, and lherzolite [*Engel and Fisher*, 1969] and the cumulate textures of some pryoxene gabbros [*Melson and Thompson*, 1970] indicate that within the crust there are layered basic complexes that have undergone gravity differentiation. This assumption is further supported by the finding of oceanic aplites [*Miyashiro et al.*, 1970*a*; *Thompson*, 1973], quartz diorite [*Bonatti et al.*, 1970], and diorite [*Aumento*, 1969], which probably represent late stages of fractional crystallization of gabbroic magma. Major element chemical analyses [*Miyashiro et al.*, 1970*a*] and trace element studies [*Thompson*, 1973] of oceanic gabbroic rocks show wide compositional variations controlled by fractional crystallization. *Miyashiro et al.* [1970*a*] have clearly demonstrated that within oceanic gabbros the decreases in the anorthite content of plagioclase are accompanied by increasing FeO*/MgO ratios, in close agreement with fractionation trends observed in many layered mafic complexes. In Figure 7 the analyses of *Miyashiro et al.* [1970*a*] are shown on

TABLE 5. Some Reported Occurrences of Gabbroic Rocks From the Oceanic Crust

Location	Petrographic Description	Reference
Mid-Atlantic ridge		
30°N	Granulated gabbros containing 40-50% plagioclase (An_{60}), 35-40% diopside, 5-8% hypersthene, 2% magnetite, and small amounts of amphibole and chlorite; altered gabbro with 40-45% labradorite, 30% diopside, and 10% hypersthene with zoisite and chlorite; anorthositic gabbro with 84% plagioclase (An_{60}), 5% diopside and bronzite, 6% amphibole, and 5% chlorite and biotite, with minor magnetite.	*Quon and Ehlers* [1963]
24°N	Tholeiitic gabbros showing strong differentiation; plagioclase composition varies from An_{47} to An_{79}; some gabbros are metamorphosed; primary hornblende is often present.	*Miyashiro et al.* [1970*a*]
1°S	Hornblende gabbro containing brown hornblende and aggregates of green amphibole, normal gabbro, olivine gabbro, and norite; mylonitized sections are common; titanomagnetite, prehnite, chlorite, iddingsite, and biotite are often present.	*Bogdanov and Ploshko* [1967]
3°S-8°N	Gabbro containing diopside, plagioclase, orthopyroxene and secondary amphibole; norite containing hypersthene, plagioclase and secondary chlorite, anthophyllite, hornblende, epidote, grunerite, and zoisite; olivine gabbro with enstatite, plagioclase, olivine, hornblende and secondary anthophyllite, talc, and chlorite; cataclastic gabbros containing clinopyroxene, plagioclase and secondary actinolite, hornblende, and chlorite; nepheline gabbro with titanaugite, plagioclase, nepheline, natrolite, aegirine, barkevikite, magnetite, and secondary chlorite.	*Bonatti et al.* [1970]
Equator	Gabbros, some of which show cumulate textures, containing plagioclase (An_{70}), augite, hypersthene, olivine(?) and secondary serpentine, chlorite, actinolite, talc, and opaques (mode of 46% pyroxene, 46% plagioclase, and 8% secondary minerals).	*Melson and Thompson* [1970]
53°N	Gabbro containing plagioclase (An_{65}), augite, orthopyroxene, olivine and secondary chlorite, serpentine, amphibole, iddingsite, and magnetite.	*Hekinian and Aumento* [1973]
Carlsberg ridge		
6°N	Granulated metamorphosed gabbro with hornblende, plagioclase (An_{50}), clinozoisite, chlorite, and sphene.	*Cann and Vine* [1966]
Tonga trench		
21°S, 173°W	Altered gabbro with plagioclase, augite and hornblende; cut by veinlets of alkali feldspar.	*Fisher and Engel* [1969]
Mid-Indian ridge		
14°S and 17°S	Coarse-grained massive gabbros at 17°S containing 63% plagioclase (bytownite), 25% augite, 5% olivine, 2% opaques, and 4% chlorite and hornblende; at 14°S one gabbro contains 67% plagioclase, 16% augite, 17% hypersthene, and minor chlorite, opaques, and antigorite; some gabbros are granulated, and others are altered to hornblende, chlorite, talc, and tremolite.	*Engel and Fisher* [1969]

a MgO-FeO*-(Na_2O + K_2O) diagram (where FeO* is total iron as FeO) along with plagioclase compositions and the fractionation trend of the Skaergaard intrusion [*Wager and Deer*, 1939].

Although hornblende gabbro, judging from its abundance in dredge hauls, is apparently an abundant constituent of the lower crust, the relationship of hornblende-bearing gabbros to cumulate gabbros is poorly understood. In many of these rocks the hornblende is clearly primary [*Miyashiro et al.*, 1970*a*; *Thompson*, 1973], whereas in others the amphiboles are secondary, having formed by uralitization and higher-grade metamorphism [*Quon and Ehlers*, 1963; *Cann and Vine*, 1966; *Engel and Fisher*, 1969; *Hekinian and Aumento*, 1973]. The latter gabbros contain primary igneous assemblages and secondary minerals formed by metamorphism and hydrothermal activity. The histories of such specimens are clearly complex; many of the reported mineral assemblages are not in equilibrium. It appears that gabbroic and metamorphic assemblages are formed in the context of high thermal gradients beneath the ridges. The lack of equilibrium often observed in these assemblages can be explained by rapid upward movement and exposure on the sea floor through faulting and diapiric intrusion or, alternatively, by rapid cooling associated with downward penetration of seawater.

Metabasites. Many rocks obtained from dredging along fracture zones and ridge median valleys that have been reported as gabbros and basalts are metamorphosed to some degree. Often, recrystallization is slight [*Miyashiro et al.*, 1970*a*], and unlike many continental metamorphics, relict igneous textures and minerals are common [*Cann and Funnell*, 1967; *Bonatti et al.*, 1970; *Miyashiro et al.*, 1971]. As is shown in Table 6, on the basis of mineralogy, metabasalts and metagabbros dredged from the ocean basins belong to the zeolite, greenschist, and amphibolite facies. The temperature of metamorphism for the higher-grade rocks must have exceeded 350°C, a value well above estimates of normal oceanic crustal temperature (calculated temperatures at the base of the crust are approximately 200°C in regions of normal heat flow). The crests of mid-ocean ridges, however, are characterized by high heat flow and high thermal gradients sufficient to produce metamorphic mineral assemblages at relatively shallow depths.

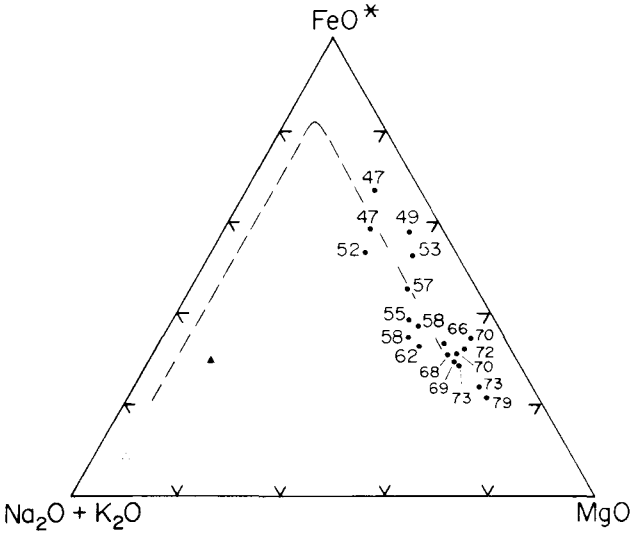

Fig. 7. A MgO-FeO*-(Na_2O + K_2O) diagram for gabbros and late differentiates dredged from the mid-Atlantic ridge at 24°N [*Miyashiro et al.*, 1970*a*; *Thompson*, 1973]. Numbers represent An content of modal plagioclase. The differentiation trend of the Skaergaard intrusion is included for comparison. Solid circles represent gabbro; solid triangles, diorite; open triangles, aplite.

Schistose and nonschistose metabasites have been reported from ridge crests and fracture zones. Although only a limited number of samples have been studied, it appears that at least in the lower-grade oceanic metamorphics the proportion of nonschistose rocks is high. Accordingly, *Miyashiro et al.* [1971] have proposed the use of the terms burial metamorphism, mid-oceanic ridge metamorphism, or ocean floor metamorphism to emphasize the poor development of schistosity.

Prehnite-pumpellyite facies assemblages are apparently rare in oceanic rocks. *Hekinian and Aumento* [1973] have described low-grade metamorphic rocks from the Gibbs fracture zone and Minia seamount that they tentatively assigned to the prehnite-pumpellyite facies. Pumpellyite has been identified in oceanic rocks by *Melson and van Andel* [1966]. *Miyashiro et al.* [1971] have reported prehnite, apparently retrograde, within a schistose amphibolite from the mid-Atlantic ridge.

Zeolite facies rocks, the mineralogies of which are summarized in Table 6, have been reported from the mid-Atlantic ridge by *Miyashiro et al.* [1971]. Although chemical changes accompanying zeolite facies metamorphism are difficult to evaluate because of the intense weathering of the rocks so far reported, metabasalts of this facies generally show Na_2O and H_2O contents higher than those of abyssal tholeiites.

Greenschist facies metabasalts and metagabbros show a wide range of mineralogy and composition. In a detailed study of the petrology and chemistry of spilites from the Carlsberg ridge, *Cann* [1969] concluded that ocean floor spilites originate from greenschist facies metamorphism of once-cooled basalt. During this process, calcic plagioclase is replaced by albite, olivine and basaltic glass are replaced by chlorite, and augite may persist metastably or form actinolite. Changes in chemistry accompanying this metamorphism involve the loss of CaO, a gain in H_2O+, and an increase in Fe_2O_3, trends similar to those produced by ocean floor weathering [*Hart*, 1970; *Hekinian*, 1971]. Intense chemical migration and albitization resulting from hydrothermal activity are common in metabasites of the greenschist facies [*Miyashiro et al.*, 1971]. It should be noted, however, that igneous plagioclase (labradorite, bytownite) is often resistant to recrystallization; hence the mineral assemblage actinolite-chlorite-calcic plagioclase is also common.

Although amphibolites appear to be common in dredge hauls from the walls of fracture zones, only a limited number have been described. Oceanic rocks belonging to the amphibolite facies are usually metagabbros, often with their original textures and chemical compositions preserved [*Cann and Funnell*, 1967; *Miyashiro et al.*, 1971]. Some oceanic amphibolites, however, have strong schistosity and well-developed banding [*Bogdanov and Ploshko*, 1967; *Bonatti et al.*, 1970; *Miyashiro et al.*, 1971]. In many samples the interpretation of the petrography is difficult because of intense mylonitization and later retrograde metamorphism [*Cann and Vine*, 1966; *Cann and Funnell*, 1967].

COMPRESSIONAL AND SHEAR WAVE VELOCITIES IN OCEANIC ROCKS

Although compressional and shear wave velocities have been reported from a wide variety of continental rocks similar to dredge samples from ridge crests and fracture zones [*Birch*,

TABLE 6. Some Reported Occurrences of Metabasalts and Metagabbros From the Oceanic Crust

Location	Facies	Mineralogy	Reference
Mid-Atlantic ridge			
30°N	Greenschist	Quartz, epidote, magnetite	*Quon and Ehlers* [1963]
1°S	Amphibolite	Hornblende, plagioclase, actinolite, leucoxene	*Bogdanov and Ploshko* [1967]
22°N	Greenschist	Albite, chlorite, epidote, actinolite, nontronite, sphene	*Melson and van Andel* [1966]
3°S-8°N	Greenschist	Albite, epidote, chlorite, actinolite, quartz	*Bonatti et al.* [1970]
	Amphibolite	Hornblende, plagioclase	
24°N and 30°N	Zeolite	Natrolite, thomsonite, analcime, chabazite, laumontite, stilbite, mixed layer chlorite-smectite + vermiculite (relict pyroxene and plagioclase)	*Miyashiro et al.* [1971]
	Greenschist	Chlorite, quartz, epidote, actinolite, plagioclase (albite and relict labradorite or bytownite)	
	Amphibolite	Hornblende, plagioclase, chlorite	
11°N	Greenschist	Chlorite, albite, actinolite, sphene	*Melson and Thompson* [1971]
4°S	Greenschist	Chlorite, albite, actinolite	*Thompson and Melson* [1972]
53°N	Prehnite-pumpellyite(?)	Chlorite, epidote, prehnite, calcite, zeolite, partially albitized calcic plagioclase, clinopyroxene, magnetite	*Hekinian and Aumento* [1973]
Carlsberg ridge			
5°N	Greenschist	Albite, chlorite, augite, sphene, actinolite, epidote	*Cann* [1969]
	Amphibolite transitional to greenschist	Hornblende, plagioclase, clinozoisite, chlorite, sphene	*Cann and Vine* [1966]
Palmer ridge			
43°N	Amphibolite	Hornblende, plagioclase	*Cann and Funnell* [1967]
Bald Mountain			
45°N, 29°W	Greenschist	Albite, epidote, tremolite, chlorite, quartz, sphene, actinolite, hornblende	*Aumento and Loncarevic* [1969]

1960, 1961; *Simmons*, 1964; *Christensen*, 1965, 1966*a*, *b*, 1968], little information was directly available from oceanic igneous and metamorphic rocks prior to 1970. Although this situation has been largely remedied, the accuracy of laboratory velocity measurements through oceanic rocks is limited by factors peculiar to their provenance. At extremely high confining pressures the velocities measured in the laboratory represent an average of the intrinsic velocities of a rock's constituent minerals. Within the range of hydrostatic confining pressures of the oceanic crust, however (0.4–2.0 kbar), most rocks exhibit significant and variable grain boundary porosity. Since velocity is strongly lowered by such porosity and is, in addition, extremely sensitive to the presence of pore fluids in grain boundary cracks, it is necessary before examining rock velocity data to examine in detail the underlying assumptions and limitations of such measurements.

Water saturation. Early studies of elastic wave propagation in sedimentary rocks [*Hughes and Kelly*, 1952; *Wyllie et al.*, 1958] and recent investigations of igneous and metamorphic rocks [*Dortman and Magid*, 1969; *Nur and Simmons*, 1969; *Christensen*, 1970*c*] have emphasized the importance of water saturation for velocities at relatively low pressures. Figure 8 shows the compressional wave velocity of a water-saturated oceanic basalt as a function of time as the sample is allowed to dry at room temperature and pressure. The decrease in compressional wave velocity is the result of slow evaporation of water from grain boundary cracks within the sample. In comparable studies the effect of water saturation on shear wave velocities has been found to be negligible [*Dortman and Magid*, 1969; *Nur and Simmons*, 1969].

At low confining pressures the increase in velocity produced by water saturation depends primarily on the rock porosity. Unweathered serpentinites have relatively low porosity and, as expected, show minimal changes in velocity with water saturation. Most oceanic igneous and metamorphic rocks, however, have significant grain boundary porosity. In Figures 9 and 10 compressional wave velocities are shown as a function of confining pressure and water saturation for typical samples of basalt from the East Pacific rise and gabbro from the mid-Atlantic ridge. Although the curves for these two samples are similar, their saturation histories are not. The basalt sample was stored in seawater immediately after dredging and received in the laboratory in its original state of saturation. The gabbro was received in a dry condition but was saturated by immersion in water following evacuation. Beyond this point, both samples have the same history. Both were cored and jacketed with copper foil to prevent the pressure medium from penetrating the samples at high pressure. A screen was placed between the sample and the jacket to allow pore fluid to drain from the sample during the application of external hydrostatic pressure (by this means, pore pressure is kept minimal). Finally, velocities were measured for a range of pressures by means of the well-known pulse transmission technique [*Birch*, 1960]. After allowing the samples to dry in the atmosphere for one week, both samples were rerun. It is clear from these two cases that not only is velocity strongly in-

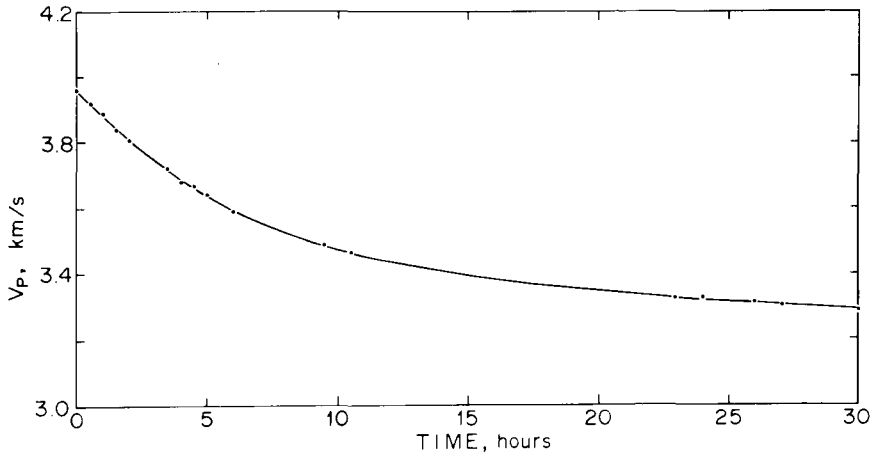

Fig. 8. Measured compressional wave velocity versus time for a sample of water-saturated basalt allowed to air dry at atmospheric pressure.

fluenced by water saturation at low pressures but also that initial conditions of water saturation can be reproduced by using laboratory techniques.

Since the range of in situ pressures within the oceanic crust is usually between 0.4 and 2.0 kbar, it is apparent from Figures 9 and 10 that the degree of water saturation of oceanic rocks constitutes an important factor that must be duplicated in the laboratory if laboratory velocity measurements are to be compared with oceanic crustal velocities. Although it has been suggested [*Fox et al.*, 1973] that the in situ interstitial water content of oceanic rocks is similar to that of air-dried laboratory samples, several independent lines of evidence suggest that it is not. Most oceanic rocks show abundant evidence of interaction with seawater, both through submarine weathering [*Hart*, 1970; *Hekinian*, 1971; *Christensen and Salisbury*, 1972] and various degrees of metamorphism in which water was an active constituent [*Miyashiro et al.*, 1971; *Cann and Funnell*, 1967; *Wenner and Taylor*, 1973]. In addition to spaces between grain boundaries, numerous fractures undoubtedly present within the oceanic crust allow water circulation. Further evidence that fractures and grain boundary cracks within the oceanic crust contain abundant water comes from studies of oceanic heat flow; measurements of heat flow on ridge crests and flanks require hydrothermal circulation as a dominant heat transfer process, since heat flow values along active oceanic ridges cannot be explained solely by conduction [*Elder*, 1965; *Deffeyes*, 1970; *Lister*, 1972]. This observation is consistent with the presence of hot springs and geysers in quasi-oceanic regions such as Iceland. Finally, the observed high electrical conductivity of the oceanic crust is most likely controlled by pore fluids [*Cox*, 1971], since most dry mafic rocks have extremely low conductivities at oceanic crustal temperatures and pressures.

Although oceanic rocks are probably saturated or nearly saturated in situ, the pore pressure of such interstitial water is not known. As was discussed by *Brace* [1971], pore pressure within crustal rocks probably varies between lithostatic, in which it balances the weight of the overlying rock and seawater, and hydrostatic, in which all pore space is continuously connected with seawater. In the course of measuring

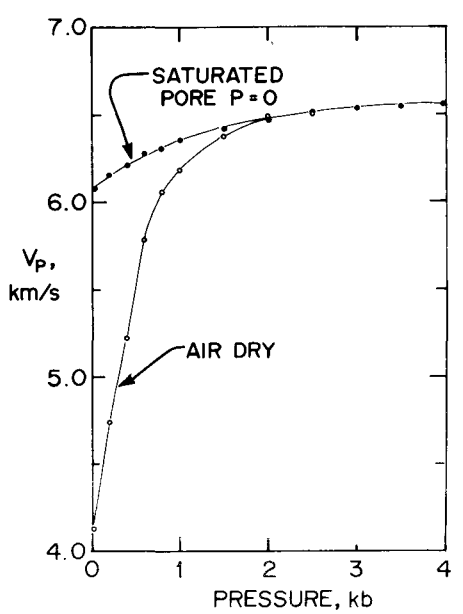

Fig. 9. Measured compressional wave velocities for air-dried and water-saturated basalt from the East Pacific rise as a function of confining pressure.

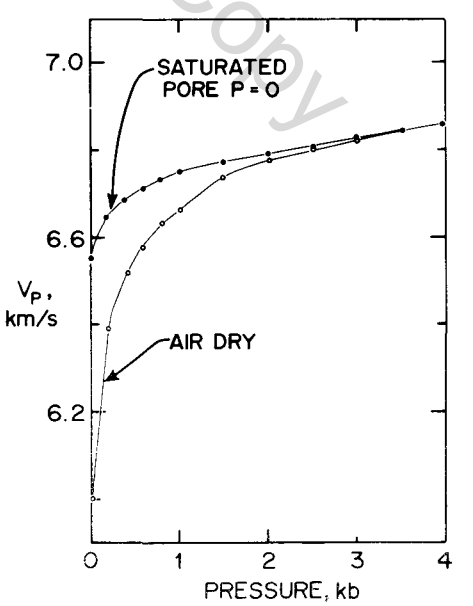

Fig. 10. Measured compressional wave velocities for air-dried and water-saturated gabbro from the mid-Atlantic ridge as a function of confining pressure.

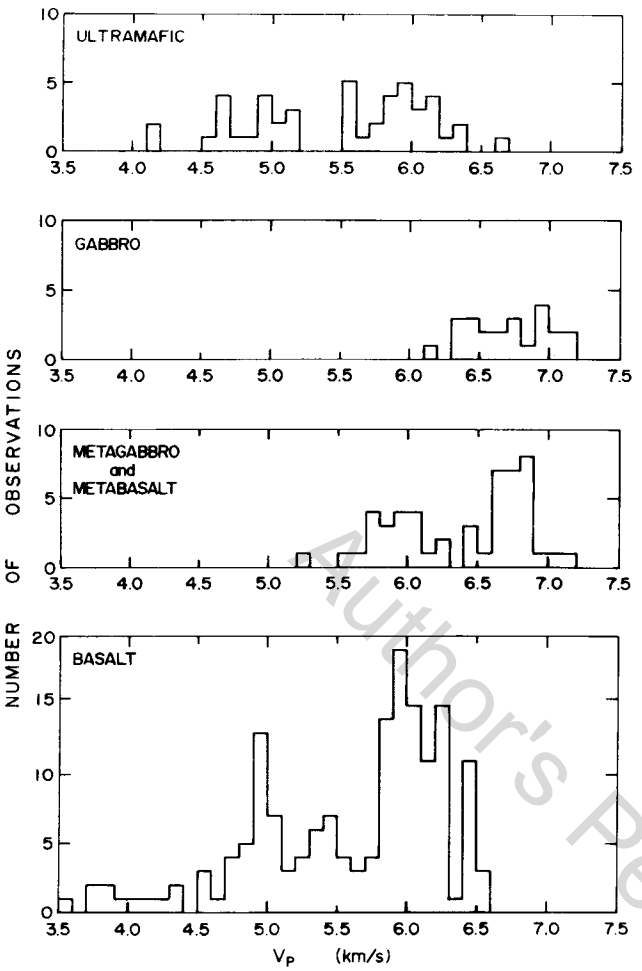

Fig. 11. Laboratory measurements of compressional wave velocity at 1 kbar for water-saturated oceanic rocks.

the velocities reported below, water was generally allowed to drain out of the rocks as confining pressure increased. To the extent that grain boundary cracks trap water during closure, experimental conditions probably produce pore pressures between lithostatic and hydrostatic values.

Ranges of velocity. A number of studies have been presented recently on seismic velocities in dredged oceanic rocks and samples collected from ophiolites. Many have been conducted over a wide range of pressures through water-saturated samples [*Barrett and Aumento,* 1970; *Christensen,* 1970*c*, 1972*a*, *c*; *Christensen and Salisbury,* 1972, 1973; *Hyndman,* 1973] and air-dried samples [*Fox et al.,* 1971, 1973; *Poster,* 1973; *Peterson et al.,* 1974]. The interested reader can find a large number of additional studies, conducted under a wide variety of experimental conditions, in *Initial Reports of the Deep-Sea Drilling Project.*

Measured compressional and shear wave velocities at a 1-kbar confining pressure for various rocks pertinent to a study of the oceanic crust are shown in histogram form in Figures 11 and 12; to make comparisons of some validity, we have included in these figures, and shall consider from this point on, velocities from water-saturated rocks only. Many of the velocities presented have been published in the references cited above. Previously unpublished data include velocities measured in our laboratory for a variety of rocks collected from the mid-Atlantic ridge [*Bonatti et al.,* 1970], the mid-Indian ridge [*Engel and Fisher,* 1969], basalts from the Lau ridge [*Hawkins et al.,* 1970], and rocks from ophiolite complexes in California [*Bailey et al.,* 1970], Oregon [*Thayer,* 1963], and Newfoundland [*Williams,* 1971].

The widest ranges of compressional and shear wave velocities are characteristic of basalts, primarily because progressive sea floor weathering causes submarine basalts to decrease in density and velocity with age [*Christensen and Salisbury,* 1972, 1973; *Hart,* 1973]. This point is illustrated in Figure 13, which shows a basalt compressional wave velocity distribution identical to the one in Figure 11 except that the velocities measured through samples less than 20 m.y. old are highlighted. Young basalts are clearly fast at the hand sample scale; basalts older than 20 m.y. old are slow. Whether this phenomenon is translated into a trend of decreasing layer 2 refraction velocities with age will depend on the depth of weathering, metamorphic overprinting, and the prevalence of such mesoscopic features as pillows, joints, and fractures.

The velocities of metagabbros and metabasalts (Figures 11 and 12) are distinctly bimodal. The lower velocities (5.2–6.3 km/s for V_p and 2.8–3.5 km/s for V_s) are typical of chlorite-rich greenschist facies rocks, whereas the higher velocities (6.4–7.2 km/s for V_p and 3.6–4.1 for V_s) are characteristic of rocks of the amphibolite facies. In all the metamorphic rocks studied the presence of chlorite was found to produce a significant lowering of velocities, whereas the presence of epidote and actinolite causes velocities to rise. The compressional

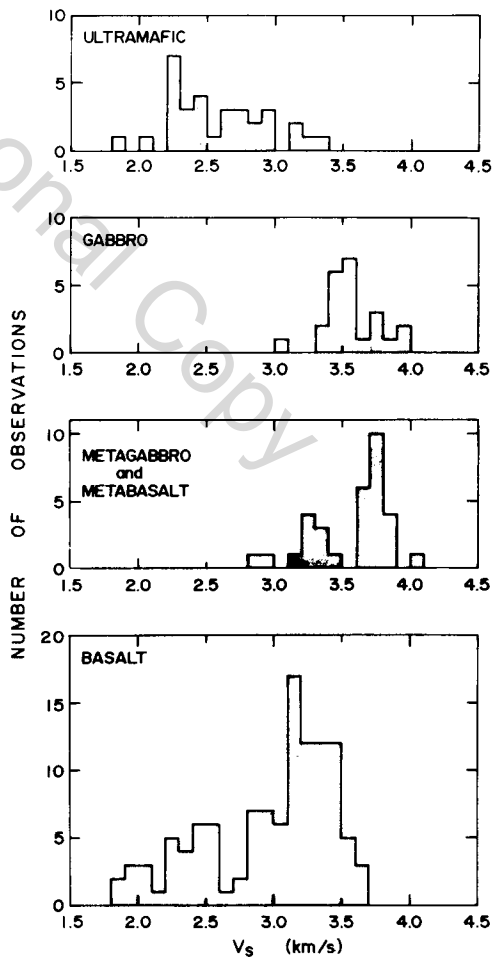

Fig. 12. Laboratory measurements of shear wave velocity at 1 kbar for oceanic rocks.

wave velocities shown in Figure 11 for greenschist facies rocks are significantly lower than the seismic velocities of the lower oceanic crust. Velocities measured to date from greenschist facies dredge samples, however, do not include many of the typical mineral assemblages characteristic of rocks described, for example, from the median valley of the mid-Atlantic ridge [*Melson and van Andel,* 1966]. Studies of velocities in continental greenschist facies rocks of equivalent mineralogy [*Christensen,* 1970*b*] show that it is possible to have greenschist facies rocks with compressional wave velocities similar to lower oceanic crustal velocities at appropriate pressures (see Table 7).

Many metamorphic rocks from dredge hauls and ophiolite complexes have significantly lower anisotropy than continental metabasalts and metagabbros. This difference is interpreted as being due to the metamorphism of oceanic rocks under conditions of low compressive stress dissimilar to those prevailing in continental orogenic regions. Nevertheless, we have found high anisotropy in some amphibolites dredged from the Vema fracture zone. An example is illustrated in Figure 14. Anisotropy in this specimen is clearly related to a strong orientation of hornblende, the maximum velocity being in the propagation direction parallel to a strong concentration of hornblende *c* axes. This anisotropy may have important implications in interpreting composition in lower oceanic crustal regions that possess seismic anisotropy [*Christensen,* 1972*b*].

The ranges of velocity shown in Figures 11 and 12 for gabbro are much less than those found for basalts, metamorphics, and ultramafics. The small number of high velocities ($V_p \simeq 7.0$ km/s, $V_s \simeq 3.8$ km/s) is characteristic of relatively fresh samples; samples that have been altered by deuteric processes or later hydrothermal activity display lower velocities.

Wide ranges of velocity in the ultramafic rocks examined are due largely to different degrees of serpentinization. Pure serpentinites have relatively low velocities; velocities increase linearly and sharply, however, with increasing density and decreasing percentage of serpentine [*Birch,* 1961; *Christensen,* 1966*b*]. As was discussed by *Christensen* [1972*a*], relatively high values of Poisson's ratio are diagnostic properties of serpentinites.

Influence of mineralogy. The influence of mineralogy on velocities and Poisson's ratio for many common oceanic rocks

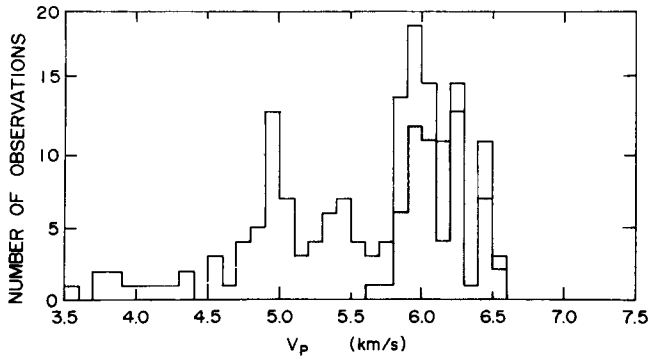

Fig. 13. Measured compressional wave velocities for oceanic basalts (from Figure 11) as a function of age. Shaded velocities are for samples from sites <20 m.y. old; the remaining sites range from 20 to 150 m.y. in age.

can be conveniently expressed by two sets of triangular composition diagrams in which the apexes are augite, hornblende, and plagioclase (An_{50}) and olivine, enstatite, and serpentine, respectively (Figure 15). Velocities measured for reasonably pure and isotropic monomineralic aggregates at 1 kbar have been selected for the end members, and contours of equal velocity and Poisson's ratio have been calculated from the velocities for intermediate points. Figure 15*a* contains mineral assemblages typical of unaltered gabbro and amphibolite. On the basis of this diagram a gabbro containing 50% plagioclase and 50% augite would have values of $V_p = 7.0$ km/s, $V_s = 3.8$ km/s, and $\sigma = 0.30$ at confining pressures of 1 kbar, similar to measured properties of several gabbros from oceanic and continental regions. Unaltered basalts of similar mineralogy have lower velocities (Figures 11 and 12) because of their finer grain size and hence greater grain boundary porosity. Amphibolites, which typically contain approximately 30% plagioclase and 70% hornblende, have values of $V_p = 6.8$ km/s, $V_s = 3.8$ km/s, and $\sigma = 0.28$. These predicted velocities again agree well with measured velocities. The plagioclase compositions of amphibolites are usually somewhat more sodic than the composition selected for Figure 15*a*, and thus the velocities would be lowered by about 0.1 km/s and there would be little effect on Poisson's ratio. The influence of mineralogy on velocities and elastic constants for rocks containing olivine, enstatite,

TABLE 7. Compressional Wave Velocity in Greenstones [*Christensen,* 1970*b*]

Sample	Density, g/cm³	Velocity V_p, km/s				
		0.4 kbar	1.0 kbar	2.0 kbar	4.0 kbar	6.0 kbar
Metabasalt						
1 (Yreka, Calif.)*	2.88	6.74	6.78	6.82	6.86	6.89
	2.90	6.80	6.85	6.89	6.93	6.97
	2.94	6.83	6.90	6.99	7.08	7.12
Mean	2.91	6.79	6.84	6.90	6.96	6.99
2 (Luray, Va.)†	2.92	6.54	6.61	6.69	6.75	6.78
	2.94	6.54	6.60	6.66	6.72	6.77
	2.93	6.47	6.54	6.60	6.66	6.71
Mean	2.93	6.52	6.58	6.65	6.71	6.75
Epidosite (Luray, Va.)§	3.17	6.19	6.72	7.04	7.18	7.24
	3.17	6.40	6.78	7.03	7.15	7.22
	3.16	6.40	6.80	7.01	7.15	7.23
Mean	3.17	6.33	6.77	7.03	7.16	7.23

*Plagioclase, actinolite, clinozoisite, chlorite, and quartz.
†Albite, epidote, chlorite, actinolite, and magnetite.
§Epidote, quartz, albite, and actinolite.

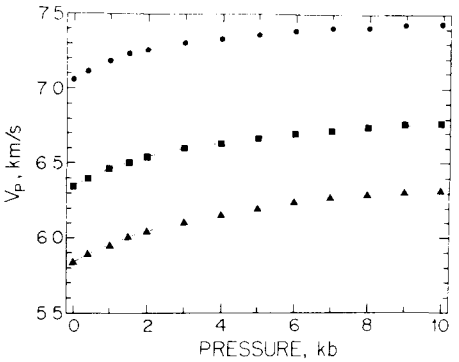

Fig. 14. Compressional wave velocities for three mutually perpendicular propagation directions in amphibolite from the Vema fracture zone.

and serpentine has been discussed in detail by *Christensen* [1966*b*]. Of significance here are the large changes in velocities and Poisson's ratio accompanying changes in serpentine content.

Velocity-density relations. Bulk densities, determined from the mass and dimensions of cylindrical samples, are almost universally reported in rock velocity studies. Relations between velocity and density are important because they allow estimates of crustal density to be made from seismic refraction velocities and, conversely, because rock densities can be used to predict elastic properties. The most frequently used velocity-density relation is that given by *Birch* [1961], in which for a given mean atomic weight the compressional wave velocity is assumed to be linearly related to density. Most samples from oceanic regions are mafic or ultramafic rocks that vary only slightly in mean atomic weight. Thus, to a first

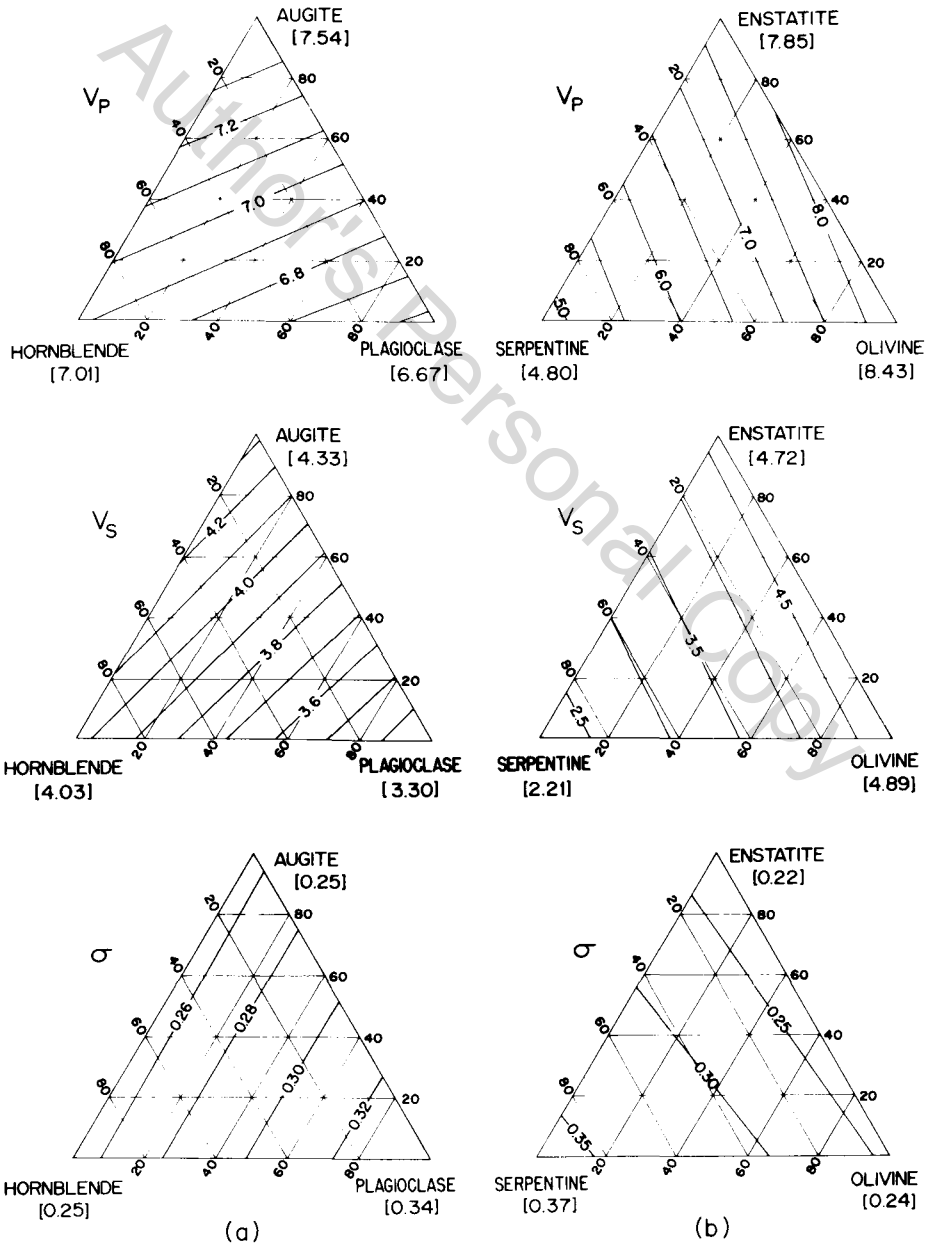

Fig. 15. Contours of constant compressional and shear wave velocity and Poisson's ratio σ at 1 kbar as a function of mineralogy in the ternary systems augite-hornblende-plagioclase and olivine-enstatite-serpentine, believed to represent lithologies common in the lower oceanic crust.

approximation, velocities of oceanic rocks should be linearly related to density. Similarly, estimates of density can be made from oceanic crustal velocities without knowledge of mean atomic weight. For this reason simple velocity-density relations are much more convenient than ones that require knowledge of rock chemistry.

In Table 8 the parameters of least squares solutions of the forms $V = a + b\rho$ and $\rho = c + dV$ are given for various groups of water-saturated oceanic rocks at pressures of 0.5 and 1.0 kbar. Owing to the lack of perfect linear correlation between velocity and density, the regression lines of V on ρ differ slightly from the regression lines of ρ on V, the latter usually having steeper slopes.

The best correlation between velocity and density is found for basalts obtained from the DSDP, as is illustrated in Figure 16. The relatively high velocities for the low-density basalts suggest that nonlinear solutions may be more appropriate than linear solutions. Thus, in Table 9, data are given in the form $V = a + b\rho^c$ for the various groups of rocks included in Table 8. The nonlinear solutions calculated for the DSDP basalts are also shown in Figure 16.

The correlation coefficients for the solutions in Table 8 that

TABLE 8. Regression Line Parameters

Solution	Pressure, kbar	n	a, km s^{-1}	b, km s^{-1}/g cm^{-3}	$S(V, \rho)$, km s^{-1}	r	r^2, %
			$V_p = a + b\rho$				
DSDP basalts	0.5	77	-4.26	3.56	0.20	0.96	93
	1.0	77	-4.10	3.52	0.20	0.97	93
All basalts except vesicular rocks	0.5	131	-4.44	3.64	0.21	0.95	91
	1.0	131	-4.44	3.67	0.21	0.95	91
All metamorphics except serpentinites	0.5	50	-3.61	3.48	0.32	0.76	58
	1.0	50	-2.79	3.22	0.31	0.74	55
All rocks except serpentinites and vesicular basalts	0.5	215	-5.06	3.91	0.32	0.90	81
	1.0	215	-4.92	3.89	0.31	0.90	81
All rocks	0.5	286	-1.34	2.60	0.42	0.83	68
	1.0	386	-1.18	2.57	0.41	0.83	68
			$V_s = a + b\rho$				
DSDP basalts	0.5	75	-3.07	2.17	0.17	0.94	89
	1.0	75	-2.79	2.08	0.15	0.94	89
All basalts except vesicular rocks	0.5	115	-3.11	2.20	0.17	0.93	86
	1.0	115	-3.07	2.21	0.17	0.93	87
All metamorphics except serpentinites	0.5	32	-3.59	2.47	0.19	0.80	64
	1.0	32	-2.89	2.25	0.18	0.78	61
All rocks except serpentinites and vesicular basalts	0.5	175	-3.66	2.43	0.23	0.89	79
	1.0	175	-3.50	2.39	0.22	0.89	80
All rocks	0.5	213	-3.36	2.32	0.25	0.88	77
	1.0	213	-3.22	2.29	0.24	0.88	77

Solution	Pressure, kbar	n	a, g cm^{-3}	b, g cm^{-3}/km s^{-1}	$S(\rho, V)$, g cm^{-3}	r	r^2, %
			$\rho = a + bV_p$				
DSDP basalts	0.5	77	1.30	0.261	0.06	0.96	93
	1.0	77	1.27	0.265	0.05	0.97	93
All basalts except vesicular rocks	0.5	131	1.36	0.249	0.06	0.95	91
	1.0	131	1.35	0.247	0.06	0.95	91
All metamorphics except serpentinites	0.5	50	1.80	0.166	0.07	0.76	58
	1.0	50	1.76	0.170	0.07	0.74	55
All rocks except serpentinites and vesicular basalts	0.5	215	1.58	0.207	0.07	0.90	81
	1.0	215	1.58	0.210	0.07	0.90	81
All rocks	0.5	286	1.22	0.262	0.13	0.83	68
	1.0	286	1.17	0.266	0.13	0.83	68
			$\rho = a + bV_s$				
DSDP basalts	0.5	75	1.56	0.407	0.07	0.94	89
	1.0	75	1.49	0.428	0.07	0.94	89
All basalts except vesicular rocks	0.5	115	1.60	0.392	0.07	0.93	86
	1.0	115	1.57	0.393	0.07	0.93	87
All metamorphics except serpentinites	0.5	32	1.96	0.258	0.06	0.80	64
	1.0	32	1.92	0.269	0.06	0.78	61
All rocks except serpentinites and vesicular basalts	0.5	175	1.78	0.324	0.08	0.89	79
	1.0	175	1.73	0.334	0.08	0.89	80
All rocks	0.5	213	1.75	0.331	0.09	0.88	77
	1.0	213	1.72	0.337	0.09	0.88	77

n is number of data points; $S_{(V,\rho)}$, standard error of estimate of V on ρ; $S_{(\rho,V)}$, standard error of estimate of ρ on V; r, correlation coefficient; r^2, coefficient of determination.

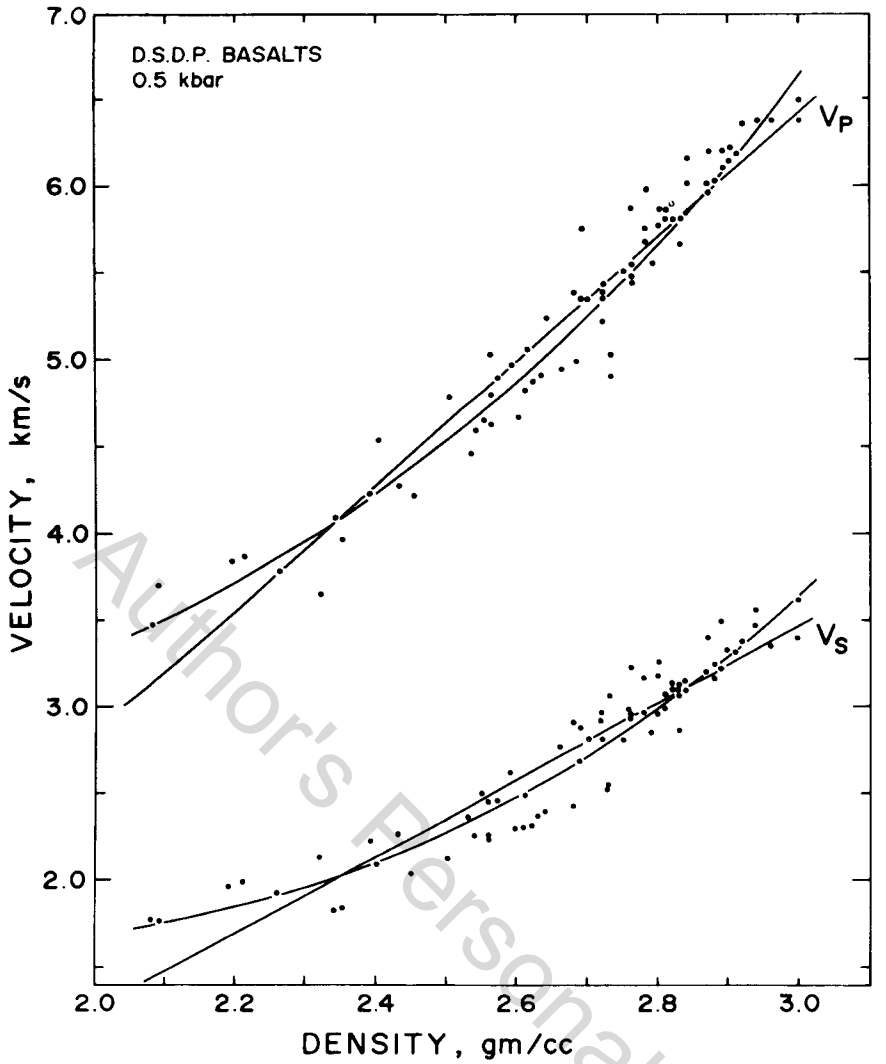

Fig. 16. Velocity-density relations for layer 2 basalts. Solutions are both linear and nonlinear.

include only metamorphic rocks are relatively low. This is interpreted as being primarily due to the presence of significant anisotropy in some of the metamorphic rocks examined.

For many of the solutions the slopes of the regression lines of V_p on ρ are between 3.5 and 3.9 km s^{-1}/g cm^{-3}. These are slightly higher than the solutions of *Birch* [1961] at 10 kbar for rocks of approximately constant mean atomic weight. Since the slopes of the regression lines of V_p on ρ commonly decrease with increasing pressure [*Christensen and Shaw*, 1970], higher slopes in Table 8 taken at 0.5 and 1.0 kbar are easily understood. An exception is noted in solution 5, in which the slope of the regression line for all rocks is only 2.6 km s^{-1}/g cm^{-3}. In Figure 17 the velocities for all rocks at 1 kbar are plotted as a function of density, together with the linear and nonlinear solutions of Tables 8 and 9 for all rocks except vesicular basalts and serpentinites. The 21 open circles with compressional wave velocities of approximately 5 km/s are measurements from relatively low bulk density high-velocity vesicular basalts from the Lau ridge. Shear velocities measured for two of these samples are shown as open circles with velocities of approximately 2.8 km/s. This figure suggests that basalt velocities are not significantly lowered by porosity arising from vesicularity (the energy follows a path of minimum travel time) and that, further, the anomalous slope of solution 5 (Table 8) is due to the relatively high velocities of vesicular basalts in relation to their bulk densities.

Velocities are also shown in Figure 17 for serpentinites and partially serpentinized ultramafics. Of importance is the fact that for a given density the compressional wave velocities for these rocks tend to be higher than velocities in gabbros, metagabbros, metabasalts, and nonvesicular basalts. Thus, as was observed earlier, the ratios of V_p to V_s and Poisson's ratio are relatively high for serpentine-bearing rocks.

The two samples in Figure 17 with the highest densities are ilmenite-rich norites dredged from the mid-Atlantic ridge. Although the presence of ilmenite in these rocks significantly increases density, compressional and shear velocities in these samples are similar to those of normal gabbros and norites. Since ilmenite-bearing norites have high mean atomic weights, these velocities are consistent with *Birch*'s [1961] observation that for rocks of the same density, velocities decrease with increasing mean atomic weight.

PETROLOGIC MODELS

A number of petrologic models have been proposed to explain the observed seismic structure of the oceanic crust. Most models assume that layer 2 consists of basalt that grades downward to low-grade metabasalt. The distributions and

TABLE 9. Nonlinear Solution Parameters

Solution	Pressure, kbar	No. of Data Points	a, km s^{-1}	b	c	Error Mean Square
		$V_p = a + b\rho^c$				
DSDP basalts	0.5	77	2.33	0.081	3.63	0.03
	1.0	77	2.37	0.085	3.57	0.03
All basalts except vesicular rocks	0.5	131	1.59	0.023	2.80	0.04
	1.0	131	1.50	0.027	2.70	0.04
All metamorphics except serpentinites	0.5	50	2.68	0.206	2.74	0.41
	1.0	50	2.93	0.165	2.73	0.43
All rocks except serpentinites and vesicular basalts	0.5	215	-0.58	1.050	1.77	0.10
	1.0	215	-0.95	1.268	1.63	0.10
All rocks	0.5	286	4.02	0.006	3.57	0.15
	1.0	286	4.10	0.007	3.49	0.14
		$V_s = a + b\rho^c$				
DSDP basalts	0.5	75	1.33	0.011	4.85	0.02
	1.0	75	1.43	0.011	4.84	0.02
All basalts except vesicular rocks	0.5	115	0.98	0.049	3.63	0.03
	1.0	115	1.11	0.040	3.79	0.03
All metamorphics except serpentinites	0.5	32	1.00	0.120	2.88	0.04
	1.0	32	1.22	0.120	2.81	0.04
All rocks except serpentinites and vesicular basalts	0.5	175	-0.09	0.311	2.27	0.05
	1.0	175	-0.02	0.319	2.24	0.05
All rocks	0.5	213	1.13	0.037	3.87	0.057
	1.0	213	1.25	0.031	3.98	0.054

relative abundances of the rock types believed to comprise the lower crust, however, are still highly debated. Having examined the seismic structure of the oceanic crust, as well as the petrology of samples recovered from the sea floor and the velocities through such samples, we are finally in a position to evaluate petrologic models of the lower crust.

Serpentinite Model

Noting the abundance of serpentinite at mid-ocean ridges and along the walls of trenches, *Hess* [1962], in a proposal that is still controversial, suggested that layer 3 is composed of serpentinized peridotite. According to Hess's model, partially serpentinized peridotite is generated by hydration of mantle peridotite along ridge crests at sites above the 500°C isotherm. Partially serpentinized peridotite, comprising layer 3, is carried laterally by sea floor spreading; the present Mohorovičić (M) discontinuity in this model represents a hydration boundary fossilized away from the ridge crests at lower temperatures of 150°–200°C. This model, later adopted by *Dietz* [1963], received considerable support when *Phillips et al.* [1969] observed that between 43°N and 43°30′N on the crest of the mid-Atlantic ridge there is an area of about 1500 km^2 in which dredging recovered serpentinized peridotite and no basalt. *Vine and Hess* [1971] suggested that within this region (which is in the vicinity of a major fracture zone and in which linear magnetic anomaly patterns are interrupted) layer 3 is directly exposed.

The first serious challenges to the concept of a partially serpentinized lower crust were presented by *Cann* [1968] and *Oxburgh and Turcotte* [1968]. *Cann* [1968] noted that (1) the supposed inverse thickness relationship between layers 2 and 3 over the mid-Atlantic ridge, observed by *Le Pichon et al.* [1965], suggests that the two layers are of similar composition, (2) the narrow range of velocities observed for layer 3 [*Raitt*, 1963] indicates a remarkably uniform degree of partial serpentinization, and (3) the absence of layer 3 over the mid-Atlantic ridge and its presence over the East Pacific rise imply that if layer 3 is composed of serpentinized peridotite, the 500°C isotherm should be within the crust under the mid-Atlantic ridge and at deeper levels under the East Pacific rise. This third point is contradicted, however, by the fact that heat flow values appear to be higher over the East Pacific rise. *Oxburgh and Turcotte* [1968], focusing on the nature of the crust-mantle transition, argued, in addition, that if the lower crust is partially serpentinized, one would expect a gradational boundary between the crust and underlying mantle. At that time, velocities in the range 7.1–7.7 km/s were not commonly

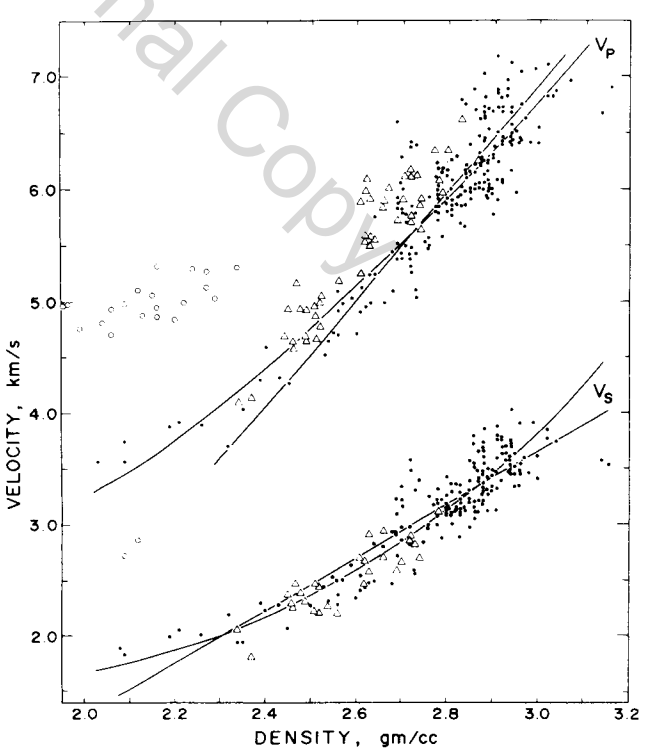

Fig. 17. Velocity-density relations for oceanic rocks at 1 kbar. Solutions are both linear and nonlinear. Open circles represent vesicular basalt; open triangles, serpentinized ultramafics.

observed in the lower oceanic crust, and it was assumed that the M discontinuity represented a sharp boundary between materials with velocities of 6.7 and 8.1 km/s. In view of these objections, Cann proposed that layer 3 is formed by metamorphism of basaltic crust to amphibolite, whereas Oxburgh and Turcotte supported the view that layer 3 is composed of gabbro or metabasite.

Le Pichon [1969] reviewed early ideas on lower crustal composition and concluded that there were no definitive arguments either for or against a serpentinite composition for layer 3. More recently, *Bottinga and Allegre* [1973], adopting a serpentinite crustal model, argued that Cann's objections to a serpentinized lower crust were erroneously based on the supposition of uniform velocities and thicknesses of layer 3 and a tenuous correlation between heat flow and layer 3 thickness. They emphasize that a considerable spread of seismic velocities is observed in the lower crust, and thus wide ranges are allowed in the degree of serpentinization. Also, because of the scatter in oceanic heat flow values, any relationship between heat flow and the thickness of layer 3 is questionable. An examination of Figures 1 and 2 shows that lower crustal velocities peak at 6.8 km/s, and it is thus suggested that peridotite of approximately 35% serpentine content may be abundant within the lower oceanic crust. However, the range of lower crustal compressional wave velocities is 6.4–7.7 km/s, which can be interpreted as evidence for variability in lower crustal serpentine content between approximately 50 and 10%. Thus uniform lower crustal velocities should not be regarded as sufficient reason for an easy rejection of a serpentinized lower crust.

The most damaging evidence against the serpentinized peridotite model for layer 3 is reported by *Christensen* [1972*a*], who shows that the ratios of V_p to V_s, and hence Poisson's ratios for partially serpentinized peridotites, are much higher than those observed from oceanic crustal seismic measurements. The dependence of Poisson's ratio on serpentine content for partially serpentinized peridotites is shown in Figure 15; a comparison of these values with the seismic data summarized in Table 1 clearly illustrates the inconsistency of measured velocities in serpentinites with layer 3 seismic refraction data. Ratios of V_p to V_s in many basaltic rocks,

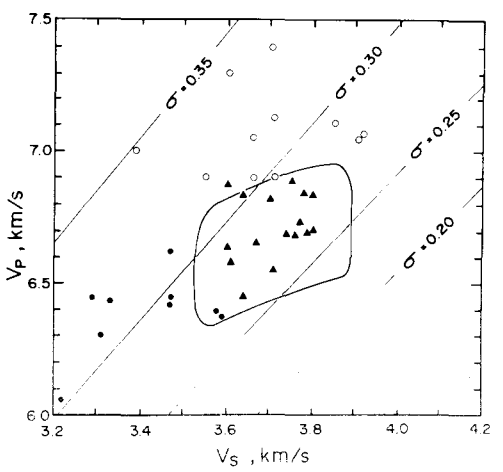

Fig. 18. Compressional and shear wave velocities at 1 kbar for possible lower crustal rocks. The shaded area shows the range of refraction velocities tabulated in Table 1. Solid triangles represent metabasite; open circles, gabbro, norite, and anorthositic gabbro; solid circles, altered gabbro and metabasite.

however, agree well with seismic observations [*Christensen*, 1972*a*]; thus it is clear that the serpentine content of the lower oceanic crust must be limited to a small fraction, probably less than 10%.

Metabasite and Gabbro Models

In addition to *Cann* [1968] and *Oxburgh and Turcotte* [1968], a number of authors have suggested that the lower crust is composed principally of gabbro or metabasite. On the basis of petrologic arguments and laboratory measurements of seismic velocities in rocks, *Christensen* [1970*a*] presented a model for the oceanic crust in which layer 3 consists of the mineral assemblage plagioclase and hornblende, occurring as hornblende gabbro and amphibolite. *Miyashiro et al.* [1970*b*] proposed that layer 3 contains metabasalt, metagabbro, and serpentinites formed by hydration of peridotites, the latter having intruded into fracture zones.

Several early papers [*Ewing and Ewing*, 1959; *Gutenberg*, 1959; *Raitt*, 1963] concerned with the seismic structure of the oceanic crust favored a simple gabbro composition for the lower crust. More recently, *Fox et al.* [1973], on the basis of a comparison of layer 3 refraction velocities with laboratory measurements of compressional wave velocities through rock samples dredged from the North Atlantic, reached this same conclusion, noting that of the oceanic rock types considered, only gabbros have velocities generally compatible with those of layer 3 (6.7–6.9 km/s) at appropriate pressures. Since we find in this study, and in earlier studies [*Birch*, 1960, 1961; *Christensen*, 1965, 1970*b*], that velocities in metabasites are, in many instances, also compatible with those of layer 3, we suggest that the composition of the lower crust is, in all probability, considerably more complex.

The principal difficulty with using only compressional wave velocities in interpreting crustal composition is that since many mineral assemblages can produce similar velocities, solutions based on this approach are nonunique. This problem is illustrated in Figure 15 for the three-component systems hornblende-plagioclase-augite and olivine-enstatite-serpentine; lower crustal compressional wave velocities ranging from 6.4 to 7.7 km/s include every possible mineral assemblage in the hornblende-plagioclase-augite system. Thus if one considers only this mineral assemblage, lower crustal compressional wave velocities can be equated with hornblendite, pyroxenite, anorthosite, amphibolite, and gabbro. Restricting consideration to velocities within the range 6.7–7.0 km/s still permits a wide variety of possible mineral assemblages to occur within the lower oceanic crust.

If both compressional and shear wave velocities are considered, however, the compositional resolution of velocity studies can be significantly improved. Unfortunately, little attention has been given by seismologists to obtaining shear velocities for crustal layers. Owing to problems in identifying and interpreting converted secondary shear arrivals characteristic of marine refraction studies, observational shear wave velocity data are extremely limited (Table 1) and subject to relatively large uncertainties. Nonetheless, the importance of these measurements in understanding crustal composition [*Christensen*, 1972*a*] makes it desirable to use what data are available.

Laboratory measurements of compressional and shear wave velocities are now available for most rock types postulated to be major constituents of the lower oceanic crust (Figures 11 and 12). In Figure 18 it can be seen that fresh gabbros, norites,

and anorthositic gabbros generally have higher Poisson's ratios and compressional wave velocities than metabasalts and metagabbros. Figure 15*a*, as was discussed earlier, also shows the variations of velocities and Poisson's ratio with mineral composition for anorthosites, gabbros, and amphibolites. Although little is known about the effect of mineralogy on the elastic properties of greenschist facies rocks, it is clear from Figures 15*a* and 18 that the metamorphism of gabbro to amphibolite facies mineral assemblages lowers Poisson's ratio to values generally between 0.26 and 0.28.

Figure 18 also shows the range of lower crustal compressional and shear wave velocities tabulated in Table 1. Although certainly more observational and experimental data are desirable, the agreement of lower crustal velocities with laboratory measurements in metabasites is striking. It should be emphasized that observed velocities are not consistent with the elastic properties of fresh gabbro. It must be noted, however, that the shear wave velocities so far determined for layer 3 are for crustal regions with compressional wave velocities of 6.5–7.0 km/s, corresponding to the upper part of the lower crustal refractor. Thus gabbro or other rock types may well be abundant constituents below the metamorphics of the lower oceanic crust.

Ophiolites

The most sophisticated and detailed models of the oceanic crust are based on examination of a small number of mafic-ultramafic complexes, the ophiolites, thought by many to be segments of oceanic crust tectonically emplaced on land. Many of the ophiolites (e.g., those of the California coast ranges [*Bailey et al.*, 1970; *Page*, 1972], Costa Rica [*Dengo*, 1962], New Caledonia [*Avias*, 1967], the eastern Celebes [*Kundig*, 1956], northern India [*Gansser*, 1964], southeast Turkey [*Rigo de Righi and Cortesina*, 1964], and the Mediterranean region [*Steinmann*, 1926; *Vuagnat*, 1963; *Pamić*, 1971]) are so faulted, dispersed, and, in some instances, metamorphosed that their examination is unprofitable for purposes of crustal reconstruction. Others (e.g., the Betts cove, Mings bight, and Baie Verte complexes of central Newfoundland) are seemingly intact but inexplicably thin [*Dewey and Bird*, 1971; *Upadhyay et al.*, 1971; *Church and Stevens*, 1971].

A small number of ophiolite complexes (in particular, the Vourinos complex of northern Greece [*Brunn*, 1956; *Moores*, 1969], the Troodos complex of Cyprus [*Bear*, 1960; *Gass and Masson-Smith*, 1963; *Gass*, 1968; *Moores and Vine*, 1971; *Greenbaum*, 1972; *Vine et al.*, 1973; *Gass and Smewing*, 1973], the Semail complex of Oman [*Reinhardt*, 1969; *Allemann and Peters*, 1972], Papua [*Davies*, 1971], and the Bay of Islands complex of western Newfoundland [*Church and Stevens*, 1971; *Williams*, 1971; *Williams and Malpas*, 1972]) are intact, unmetamorphosed, and, in the last three instances, stratigraphically robust. Although they are subject to other interpretations, it has been suggested that the Troodos and Papuan complexes can be geophysically traced to the sea [*Gass and Masson-Smith*, 1963; *Davies*, 1971], a distinction shared only with the Macquarie Island ophiolite complex [*Varne et al.*, 1969; *Varne and Rubenach*, 1972], which is apparently being raised above sea level even at the present time.

The stratigraphic columns representing this select group of ophiolites are presented in Figure 19, along with Raitt's mean oceanic crust and the mean of each velocity model obtained from the sonobuoy data presented earlier in Figure 6. Lithologic, structural, textural, and metamorphic facies relationships observed in these complexes have been incorporated in Figure 19 to facilitate comparison with samples dredged and cored from the oceanic crust and to facilitate interpretation in terms of seismic structure. It should be noted that since these complexes are the subject of current study, their columns are subject to revision. For each ophiolite in Figure 19 the lower crustal refractor has been equated with diabase dikes when they are present in sufficient number. As was shown in the preceding section, the top of the refractor is most likely a boundary dependent on metamorphic grade. Thus the actual position of this boundary may be within the dike swarms.

Ultramafics of the ophiolite column. The ophiolites in Figure 19 are, in many respects, remarkably similar. The deepest level of each consists of a thick unit of ultramafic tectonite composed of harzburgite, dunite, and lherzolite lying in fault contact against country rock. Where the basal contact is exposed, the country rock generally is observed to have a metamorphic 'aureole' of garnet amphibolite in the vicinity of the fault. The uppermost levels of the ultramafics appear to be generally, although not invariably, cumulate in origin. This level exhibits a wide variety of ultramafic lithologies, dunite, harzburgite, and pyroxenite predominating. Cumulate or podiform chromitites are commonly associated with the dunites. Pyroxenites, abundant in the ophiolites only at this level and in the lower levels of the overlying gabbros, tend to be clinopyroxene rich (augite, chrome diopside), as are associated peridotites. The uppermost ultramafics are usually feldspathic peridotites or feldspathic dunites, signaling the first appearance of feldspar as a cumulus phase and the transition to the overlying gabbroic level.

The transition zone or 'Moho' between the ultramafics and the gabbros is often strongly layered with dunite, pyroxenite, anorthosite, feldspathic dunite, wehrlite, norite, and troctolite as the predominant lithologies.

Significantly, the transition zone is often quite abrupt (for example, in the Bay of Islands complex the change from olivine to calcic plagioclase as the predominant cumulus phase occurs in less than 100 m). Finally, the transition zone and the levels adjacent to it are commonly intruded by dikes and pegmatites of pyroxenite, anorthosite, and gabbro.

Gabbros. The thick gabbroic level above the ultramafics, commonly equated in whole or in part with layer 3 [*Gass*, 1968; *Dewey and Bird*, 1971; *Moores and Vine*, 1971], can best be described in terms of three major elements present in varying degree in the ophiolites of Figure 19: cumulate gabbros, massive gabbros, and gabbroic sheeted dikes.

Cumulate gabbros are found, and in many instances are predominant, in the lower levels of each complex shown in Figure 19. Near the Moho transition zone, pyroxenites, troctolites, and anorthosites are common, but upward the cumulate gabbros are for the most part noritic; near the top of the cumulates, gabbros with primary and, in some instances, cumulate hornblende are often encountered. Although layering, particularly in the lower levels, is often extremely well developed, individual layers cannot usually be traced laterally for more than a few hundred meters. The cumulate gabbros grade upward and/or laterally into massive gabbros. With the exception of Papua, where the gabbros are hornblende free, the massive gabbros are often extensively uralitized and saussuritized. In both the cumulate and noncumulate cases the differentiation in the gabbros is extensive: not only do the gabbros become increasingly silica rich upward but also the

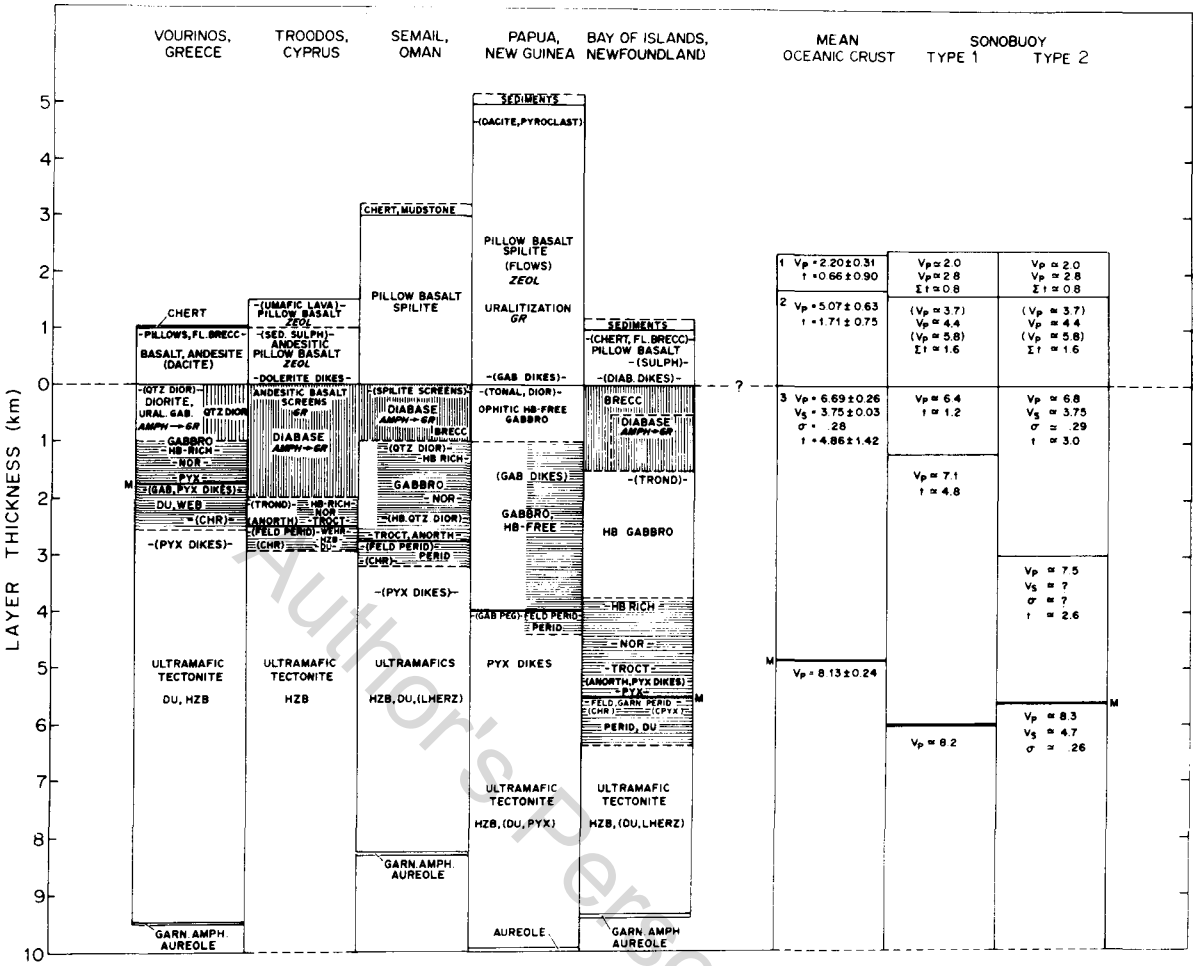

Fig. 19. Comparison of stratigraphic and petrologic field relations in major ophiolite complexes with the seismic structure of the oceanic crust as summarized by *Raitt* [1963] and interpreted from sonobuoy studies. Minor lithologies are in parentheses; lithologies of limited vertical range are between dashed lines; metamorphic facies terms are in italics. Vertical and horizontal striping represents sheeted dikes and cumulate layering, respectively.

petrologic extremes of mafic differentiation, namely, diorites, trondhjemites, and granophyres, are usually found as pods and intrusions at structurally high levels just below the sheeted dikes.

The last and most intriguing element of the gabbroic level is the sheeted dike complex found in the upper levels of four of the five ophiolites examined here. Many authors [*Bear*, 1960; *Gass and Masson-Smith*, 1963; *Moores and Vine*, 1971] consider that these complexes, consisting in the most well-developed instances entirely of narrow one-sided vertical dikes intruded one against the next with no country rock, could have been formed only in a tensional environment such as that thought to exist at ridge crests. This configuration is persuasive and nearly unique to the ophiolites but not ubiquitous among them, being absent, for example, in Papua and only poorly developed in Vourinos.

Viewed more closely, the sheeted dikes are quite complex. Their lower contact is characterized by mutually contradictory (i.e., synchronous) intrusive relations in which the sheeted dikes intrude and are intruded by the underlying massive and cumulate gabbros. In some instances (e.g., Troodos) highly metamorphosed vestiges of extrusive country rock are present as screens. The contact with the overlying extrusive unit is equally complex, being best described in a statistical sense as that point at which the dikes, diminishing in number upward, first constitute less than 50% of the unit. Also, at approximately this point in many complexes the remaining dikes continue upward as feeders for extrusives at higher levels and become more randomly oriented.

The dikes themselves are also internally complex. Many are brecciated [*Reinhardt*, 1969; *Williams and Malpas*, 1972] by a mechanism tentatively identified as gas fluidization. In addition, there appear to be several stages of dike intrusion. Finally, it should be noted that of the minerals originally present in the sheeted dikes, only altered plagioclase and minor relict pyroxene remain, the pyroxene having been partially or completely replaced by hornblende characteristic of the amphibolite facies or by fibrous actinolite of the greenschist facies [*Williams and Malpas*, 1972; *Varne and Rubenach*, 1972]. The metabasites of the sheeted dikes, and in some instances the massive gabbros below, often show evidence of having been pervasively uralitized and sausseritized, apparently through extensive hydrothermal metamorphism.

Extrusives. Overlying the gabbros in all the ophiolites examined is a unit of igneous extrusives composed of pillows, flows, and minor flow breccias of basaltic or andesitic composition. Greenschist facies spilites are common in the lower levels of particularly thick extrusive piles; high-level extrusives are generally in the zeolite facies. Sulphide mineralization is common and apparently associated with late-stage intrusive

activity. Ultramafic extrusives are reported but rare [*Gass and Masson-Smith,* 1963].

Sediments. Intercalated in and lying depositionally upon the extrusives are often found cherts of deep-sea origin, shales, and, in some instances, clastics from the continental margin. These represent the uppermost and final unit of the ophiolites.

Evaluation of the ophiolite hypothesis. Although the ophiolite model of oceanic crustal structure has been presented in some detail above, a question remains: what evidence is there both for and against the hypothesis that the ophiolites are segments of oceanic crust? In response to this question the following arguments can be presented in support of the hypothesis.

1. Cherts and shales forming an integral part of many of the ophiolites are clearly of deep-sea origin.

2. The presence of pillow structures in the extrusives demonstrates formation in a subaqueous environment. That these extrusives are frequently spilites suggests (but does not prove) that this environment was oceanic.

3. There is an excellent correspondence between lithologies obtained in dredge hauls at sea, described in the section on rocks from the lower oceanic crust, and those observed and described above for the ophiolites. This correspondence incorporates not only all major lithologies and metamorphic facies but also extends even to obscure lithologies such as plagioclase peridotite [*Ploshko and Bogdanov,* 1968; *Smith,* 1968], hydrogrossular peridotite [*Switzer et al.,* 1970; *Smith,* 1958], anorthosite, troctolite, and granophyre. As well as can be determined, there is also a rough correlation between the stratigraphic position of a given lithology in the ophiolites and its recovery interval in dredging [*Bonatti et al.,* 1970].

4. If seismic velocities are assigned to the ophiolites on the basis of the observed lithologies discussed above and the laboratory findings presented earlier, the velocity column of the ophiolites is found to be consistent with that of the oceanic crust as determined from seismic refraction studies. Specifically, the extrusives will range in compressional wave velocity V_p between 3.5 and 6.5 km/s (identical to the range of layer 2 velocities) and in shear wave velocity V_s between 1.8 and 3.6 km/s. The lowest velocities will be noted in extremely weathered or pillowed extrusives, the highest velocities in fresh basalts, and intermediate velocities in chlorite-rich greenschist facies metabasalts and moderately weathered or pillowed extrusives.

Velocities in the gabbroic unit will range, on the basis of laboratory studies, from 6.3 to 7.2 km/s for V_p and from 3.3 to 4.0 km/s for V_s, in good agreement with the observed range of velocities for layer 3. In the uppermost, or sheeted dike, level the compressional and shear wave velocities will be those of hornblende metagabbro, 6.8 and 3.8 km/s, respectively. Unmetamorphosed and cumulate gabbros found at intermediate levels will have compressional wave velocities of 7.0–7.2 km/s in the horizontal propagation direction and, in the case of cumulate gabbros, may have velocities as high as 7.4 km/s in the vertical direction owing to the statistical alignment of plagioclase [010] axes in the vertical direction during crystal settling. Since the [010] direction in plagioclase is fast [*Alexandrov and Ryzhova,* 1962; *Ryzhova,* 1964], cumulate gabbros are transversely isotropic, velocities being slow in the horizontal plane of refraction propagation. Although measured velocities in selected directions in cumulate gabbros may approach those of the basal layer of *Sutton et al.* [1969], it is apparent that the velocity of the basal layer cannot be explained in terms of this lithology. Only in the very mafic lower levels of the cumulates, in the vicinity of the gabbro-ultramafic transition zone, are lithologies encountered with compressional wave velocities comparable to those of the basal layer.

Since layer velocities are determined from energy propagating along the uppermost part of a layer, layer 3 velocities in ophiolites should correlate with sheeted dike metamorphic assemblages rather than with the underlying gabbro. It is thus significant that the compressional and shear wave velocities of these assemblages are in specific agreement with those of layer 3. It is also interesting to note that petrologic models equating layer 3 with gabbro on the basis of velocity are thus inconsistent with ophiolite models.

Finally, on the basis of velocity measurements through unserpentinized ultramafics reported elsewhere in the literature [*Birch,* 1960; *Christensen,* 1966*b*], the mantle level of the ophiolites will range in compressional wave velocity from 7.8 to 8.5 km/s, in good agreement with measured oceanic mantle velocities.

5. Internal structural relations in the ophiolites are consistent with formation at the ridge crests. Specifically, the presence of sheeted dikes and cumulates implies continuous creation of void space at a site of tensional spreading; the filling of this space with tholeiitic magma suggests that this site was in the ocean basins.

6. Finally, the high heat flow commonly observed at the ridge crest cannot be explained by thermal conductivity alone; as was demonstrated by *Bottinga* [1974] and *Lister* [1972], a large additional component of heat transfer must occur through water circulation to considerable depths in layer 3. An almost inevitable consequence of such circulation would be pervasive hydrothermal metamorphism comparable to the uralitization, sausseritization, and spilitization observed in the extrusives and upper gabbros of the ophiolites. Where water has been denied access to the lower oceanic crust, as perhaps it has in Papua, such metamorphism would be lacking or incomplete.

Although many features of the ophiolites can best be explained in terms of an oceanic crustal origin, a disconcerting number of features remain inconsistent with the ophiolite hypothesis.

1. Although seismic velocities measured for the ophiolite columns are consistent with those of the oceanic crust, thicknesses, for the most part, are not. Of the five ophiolites examined in Figure 19, only one, the Bay of Islands complex, has both an extrusive layer and a gabbroic layer with thicknesses falling simultaneously within one standard deviation of Raitt's mean thickness estimates for layers 2 and 3. Layer 3 thicknesses for most of the ophiolites, including such petrologically complete complexes as Troodos [*Gass and Masson-Smith,* 1963], Canyon Mountain [*Thayer,* 1963], Vourinos [*Moores,* 1969], Semail [*Reinhardt,* 1969], Mings bight, Baie Verte, and Betts cove [*Dewey and Bird,* 1971], are thin by factors ranging from 2 to 5.

In addition, in no ophiolite has a basal layer of reasonable thickness been found. Recently, *Moores and Jackson* [1974] have equated the basal layer of *Sutton et al.* [1971] to layered cumulates found in the lower sections of ophiolites. The lower-velocity basal layers ($V_p \simeq$ 7.1–7.2 km) are postulated to originate from the presence of olivine cumulate containing as much as 25% plagioclase and 25% pyroxene in the interstices,

and higher-velocity basal layers (~7.6 km/s) are presumably composed of olivine cumulate with less postcumulus material. Simple calculations based on mineral and rock velocities summarized by *Birch* [1960, 1961] and *Christensen* [1965] show that at 2 kbar a rock containing 50% olivine, 25% pyroxene, and 25% plagioclase (An_{80}) would have a compressional wave velocity between 7.8 and 8.0 km/s. Since velocities increase with decreasing pyroxene and plagioclase content, the rocks described by *Moores and Jackson* [1974] cannot be crustal constituents but, on the basis of velocity, belong within the upper mantle ($V_p \simeq 7.8$–8.5 km/s). Lithologies, however, that would produce acceptable basal layer velocities are olivine gabbro [*Christensen*, 1965], partially serpentinized peridotite [*Birch*, 1960, 1961; *Christensen*, 1966*b*], pyroxenites [*Birch*, 1960], and foliated amphibolites [*Christensen*, 1965].

2. Major parts of the extrusive levels of several of the ophiolites (for example, Vourinos and Troodos) are composed not of oceanic tholeiites but of andesitic basalts and andesites [*Moores*, 1969; *Moores and Vine*, 1971]. This composition has prompted *Miyashiro* [1973] to suggest that many of the ophiolites were formed not on the ridge crest but in an island arc environment.

3. Values of heat flow measured at the ridge crests are too low to be consistent with the existence of magma chambers in layer 3 of the size considered necessary to generate major cumulate complexes [*Bottinga and Allegre*, 1973].

4. Sediments interbedded with and immediately overlying the uppermost extrusives of a number of the ophiolites are not of deep-sea origin but are characteristic instead of the continental margin or island arc environment [*Dewey and Bird*, 1971].

5. In the case of at least two of the ophiolites (Troodos and the Bay of Islands) the orientation of the sheeted dikes is currently perpendicular, rather than parallel, to the trend of the ridge crests at which they are thought to have been formed [*Moores and Vine*, 1971; *Williams and Malpas*, 1972].

6. If the M discontinuity lies at a transition between cumulate gabbro and cumulate ultramafics, as it does in the ophiolites [*Moores and Vine*, 1971], mantle refraction velocities will be from cumulate ultramafic levels. This supposition is inconsistent with observed mantle anisotropy, since cumulate ultramafics are, for the most part, transversely isotropic [*Christensen and Crosson*, 1968].

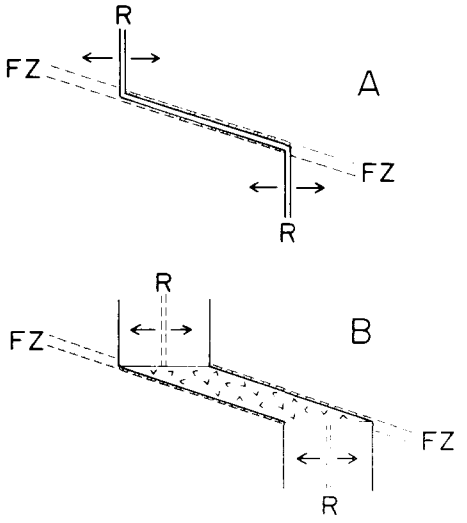

Fig. 20. Formation of new oceanic crust in leaky transform fault zones as a result of a change in the spreading direction [*van Andel et al.*, 1969].

The objections raised above do not argue against an oceanic origin for the ophiolites but emphasize that the ophiolites are not normal oceanic crust. Where, then, might they originate? Three sites answer, in part, this question and the objections raised above.

Marginal basins, leaky transform faults, and immature ridge crests. A number of authors [*Dewey and Bird*, 1971; *Upadhyay et al.*, 1971] have suggested that some ophiolites originated in marginal basins. Such an origin might well explain the andesitic nature of some ophiolite extrusives; rocks of this suite have been recovered, for example, from layer 2 in the Philippine Sea [*Karig*, 1972]. Such an origin is also consistent with the presence of volcano clastic sediments and tuffs typical of marginal basin deposits [*Ingle et al.*, 1973] immediately above some ophiolite extrusives. Still left unexplained, however, is the anomalously thin crust of the ophiolites.

Recent discussions of the composition of the oceanic crust have usually been based on the assumption that crust in the main ocean basins is generated almost entirely along a fairly narrow zone parallel to the ridge crests. Recently, *van Andel et al.* [1969] have proposed a model by which significant amounts of oceanic crust might be formed within fracture zones. This model, as developed for the Vema fracture zone, is illustrated in Figure 20. The initial stage of the opening of a fracture zone requires reorientation of plate movements; for the Vema fracture zone this change is from E10°S to E-W. Following this reorientation, progressive spreading produces an opening rift along the old fracture zone that acts as a site for the emplacement of new crust.

Thompson and Melson [1971] noted several additional fracture zones in the Atlantic in which crust might be forming by this same mechanism. They further attach significance to the alkaline character of many rocks emplaced within these faults, suggesting that oceanic crust formed along leaky transform faults may be different from that formed at ridge crests. In regard to the ophiolites, it may also be significant that the crust in fracture zones is commonly thin and that sheeted dikes formed in such an environment would be perpendicular to the regional trend of the ridge.

Since young crust at ridge crests is commonly thin but thickens with age to 40 m.y. (Figure 4), it follows that the ophiolites may be segments of immature oceanic crust, emplaced on land before reaching normal oceanic crustal thickness. This hypothesis can easily be tested by determining (Table 10) the difference between the time of formation and the time of emplacement for each ophiolite (i.e., the age at the time of emplacement). As can be seen, the ophiolites were invariably young when they were emplaced.

The youth of the ophiolites imposes a considerable restraint on possible mechanisms of emplacement. It is proposed that the most likely mechanism consistent with this phenomenon is the one shown in Figure 21. During the closure of any ocean basin through subduction of one or both of its limbs the ridge crest itself must at some point be subducted. This point is unique in that for the first and only time a thin hot mechanically weak segment of oceanic crust and upper mantle, laced with magma chambers, is presented to the subduction mechanism. That subduction of the ridge crest occurs without incident is unlikely. It is anticipated, rather, that the ridge crest will be dismembered by faulting, major segments, particularly from

TABLE 10. Time Relationships in Some Major Ophiolite Complexes

Location	Time of Formation	Time of Emplacement	Age at Time of Emplacement, m.y.	Reference
Troodos, Cyprus	Lower Campanian	Lower Campanian	<5	*Gass* [1968], *Moores and Vine* [1971], *Vine et al.* [1973]
Vourinos, Greece	Neocomian-Tithonian	Pre-Cenomanian	<35	*Moores* [1974]
Semail, Oman	Cenomanian-Turonian	Lower to middle Maaestrictian	20-30	*Allemann and Peters* [1972]
Papua, New Guinea	Upper Cretaceous	Upper Eocene or Oligocene	35-55	*Davies* [1971]
Bay of Islands, Newfoundland	Arenigian	Middle Ordovician	25	*Williams* [1971]
Macquarie Island, Macquarie ridge	Early to middle Miocene	Present	<20	*Varne and Rubenach* [1972]
Trinity, Calif.	Lower Ordovician	Upper Ordovician	20	*Hopson and Mattinson* [1973]

the upper levels of the outboard plate, being obducted onto the continental margin while the inboard plate is depressed under the approaching continental plate and subducted. Besides being young and thin, ophiolites formed in such a manner would also be expected to (1) have a minimal cover of sediments of pelagic origin, the overlying sediments being composed instead of trench or continental margin deposits, (2) display, at least in some instances, evidence that their upper levels were still partially molten during emplacement, (3) have metamorphic aureoles at their bases, and (4) thin toward the continental block. All these features have, in fact, been observed. Still unexplained, however, is the andesitic composition of the extrusives. In some ophiolites this would no longer pose a problem if the spreading ridge were in a marginal basin.

Finally, it should be noted that if ophiolites are from the ridge crest province, comparison of ophiolite lithologies with those dredged from the fracture zones may be valid, but neither suite is from normal oceanic crust in that both sites are young. It follows that ultramafic tectonites may be from the anomalous mantle; whether they were tectonized during emplacement or not, their fabrics may not be representative of the fabric of the normal oceanic mantle.

SUMMARY AND CONCLUSIONS

Within the framework of Raitt's synthesis of the mean seismic structure of the oceanic crust, patterns of refraction data suggesting regional and local structural differences, seismic anisotropy at intermediate crustal levels, and evolution of seismic structure with age are beginning to emerge.

In a 15-m.y.-wide band to either side of the ridge crest, more than 50% of the sites examined by refraction techniques are floored by anomalous mantle ranging in velocity V_p between 7.2 and 7.8 km/s; layer 3 at these sites is either absent or, if present, thin but of normal velocity (6.8 km/s), whereas layer 2 is somewhat thickened at sites in which layer 3 is missing. The observation of high heat flow and the attenuation of shear waves observed at the ridge crests imply the existence of high-temperature intrusions, and it is thus suggested that the thickening of layer 2 at those sites in which layer 3 is absent may be due to thermal depression of velocities in layer 3 material. At ridge crest sites displaying normal mantle velocities, layer 2 is usually normal, and layer 3 is again thin. Mantle anisotropy appears to be absent to weakly developed [*Whitmarsh*, 1971].

Beyond 15 m.y., sites with anomalous mantle velocities are rare, but mantle anisotropy becomes pronounced, V_p becoming fast ($\simeq$8.3 km/s) perpendicular to the ridge crest and slow ($\simeq$8.0 km/s) parallel to the ridge crest. Layer 3 thickens rapidly away from the ridge crest, reaching a full thickness of approximately 5 km at 40 m.y. Unexpectedly, layer 3 velocities change slowly with age. Velocities of 6.8 km/s, characteristic of layer 3 at the ridge crest, are virtually absent in crust over 80

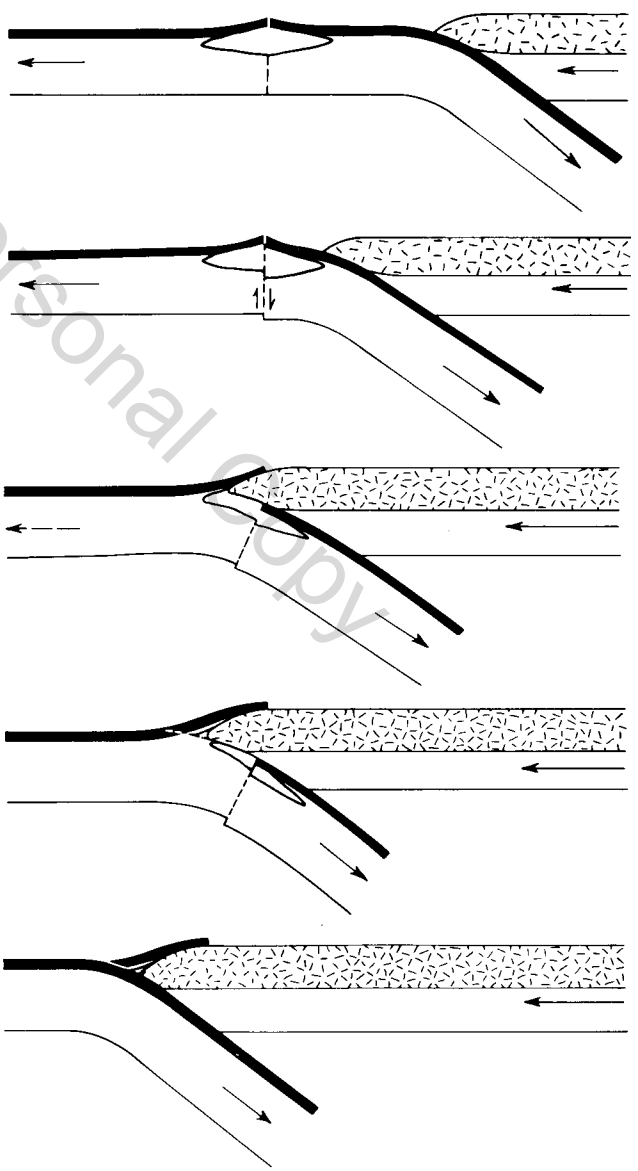

Fig. 21. Ophiolite emplacement during subduction of a ridge crest.

m.y. old, being replaced by a bimodal distribution of velocities with peaks at 6.5 and 7.0 km/s. Also unexpectedly, layer 3 is statistically anisotropic, being slightly faster parallel to the ridge crest than it is perpendicular to the ridge crest.

Differences in seismic structure associated with tectonic province are difficult to delineate at this time owing to poor statistics. Nonetheless, a number of gross features can be outlined. (1) The crust of fracture zones appears to be conventionally three layered but thin; layer 2 velocities are invariably low, presumably owing to brecciation. (2) The crust of offridge rises, back arc rises, and linear island chains is anomalously thick; in the first two instances this excess is distributed within a conventional three-layer structure; in the third, layer 2 is multilayered and two to three times normal thickness, whereas layer 3 is normal in thickness but depressed in velocity. The crust of trenches, troughs, and back arc basins is distinguished only by exceptionally thick sediments.

Finally, the oceanic crust may be divided locally, though not invariably, into at least two structural types based on layer 3 subdivisions detected through sonobuoy studies: type 1, in which layer 3 consists of a thin 6.4-km/s upper level underlain by a thick 7.1-km/s level, and type 2, in which layer 3 consists of two subdivisions of equal thickness, an upper 6.8-km/s level and a 'basal layer' of 7.5 km/s.

The velocity structure of the oceanic crust must ultimately be explained in terms of lithologies dredged from the ocean floor. Within these lithologies (Table 11) are metamorphic rocks of low to intermediate grade and igneous rocks that show evidence of crystal fractionation. In all cases the rocks are predominantly mafic.

Laboratory velocity measurements conducted on dredge samples representing these lithologies show, under conditions of confining pressure and water saturation appropriate to the oceanic crust, the distinctive velocity patterns summarized in Table 12. From this table it is apparent that layer 2 is composed of basalt and probably chlorite-rich metabasite of either basaltic or gabbroic origin. Of the three petrologic models currently proposed in the literature for layer 3 (namely, that layer 3 is composed of either partially serpentinized ultramafics, gabbro, or metabasite), two may be dismissed upon consideration of laboratory and refraction velocity measurements. Compressional and shear wave velocities in partially serpentinized ultramafics are, for the most part, much lower than velocities observed for layer 3; those samples with comparable compressional wave velocities are still incompatible in V_s and σ. Shear wave velocities in normal gabbro (3.8 km/s) are similar to those of layer 3 ($\simeq$3.75 km/s), but measured compressional wave velocities from unmetamorphosed samples (7.0 km/s) are too high. Of the common oceanic lithologies, only hornblende-rich metabasites seem to have values of V_p and V_s that are both consistent with those of layer 3. A model of layer 3 composition based on this lithology alone, however, is incomplete in view of the presence of unmetamorphosed gabbros among the recovered lithologies listed in Table 11. It is thus proposed that hornblende metagabbros predominate in the upper levels of layer 3 sampled by refraction but that unmetamorphosed gabbros predominate at deeper levels.

This relationship is implied in Table 11, which is itself a petrologic model of the oceanic crust constructed simply by listing observed dredged lithologies according to the following premises. (1) Extrusives (and sediments) overlie intrusives. (2) Metamorphic grade increases with depth. (3) In high-temperature facies exhibiting differentiation and cumulate textures the lithologic order is determined by the crystallization order. This model incorporates dredged lithologies into an internally consistent petrologic framework that is, at the same time, consistent with observed refraction and laboratory measurements of seismic velocity. By leaving this model unscaled, the wide range in seismic structure observed in the

TABLE 11. Lithologies Reported From the Sea Floor

Layer	Lithology	
1	Sediments	
2	Tholeiitic basalt (weathered to fresh)	
	Metabasalt*	metabasites
3	Metagabbro†	metabasites
	Amphibolite (schistose and nonschistose)	metabasites
	Aplite	
	Quartz diorite	
	Diorite	
	Nepheline gabbro	
	Primary hornblende gabbro	
	Gabbro	some with cumulate textures
	Two-pyroxene gabbro	some with cumulate textures
	Norite	some with cumulate textures
	Anorthositic gabbro	some with cumulate textures
	Anorthosite	some with cumulate textures
	Olivine gabbro	some with cumulate textures
	Troctolite	some with cumulate textures
Mantle	Picrite	some with cumulate textures
	Plagioclase peridotite	
	Dunite	as serpentinites, partially serpentinized peridotites
	Harzburgite	as serpentinites, partially serpentinized peridotites
	Lherzolite	as serpentinites, partially serpentinized peridotites

*Includes zeolite facies, prehnite-pumpellyite facies (rare), and greenschist facies (spilite).
†Includes greenschist facies and amphibolite facies.

TABLE 12. Summary of Laboratory Velocity Measurements on Oceanic Rocks (1 kbar)

Lithology	V_p, km/s		V_s, km/s	
	Range	Average	Range	Average
Basalts (weathered to fresh)	3.7-6.5	5.5	1.8-3.6	2.9
Metabasites				
Chlorite rich	5.2-6.3	5.9	2.8-3.5	3.2
Amphibole rich	6.4-7.2	6.8	3.6-4.1	3.8
Gabbro (fresh, unmetamorphosed)	6.9-7.2	7.0	3.6-3.9	3.8
Ultramafics (serpentinized)	4.1-6.6	5.5	1.8-3.3	2.6

oceanic crust can be attributed to variation in thickness at any level, together with vertical displacements of metamorphic facies boundaries. It is interesting to note that a strong but discontinuous velocity inversion can be predicted in layer 3 wherever low-velocity late differentiates underlie amphibole-rich metabasites and in layer 2 wherever chlorite-rich metabasalts are overlain by fresh unpillowed basalts.

Although this model is consistent with structural and

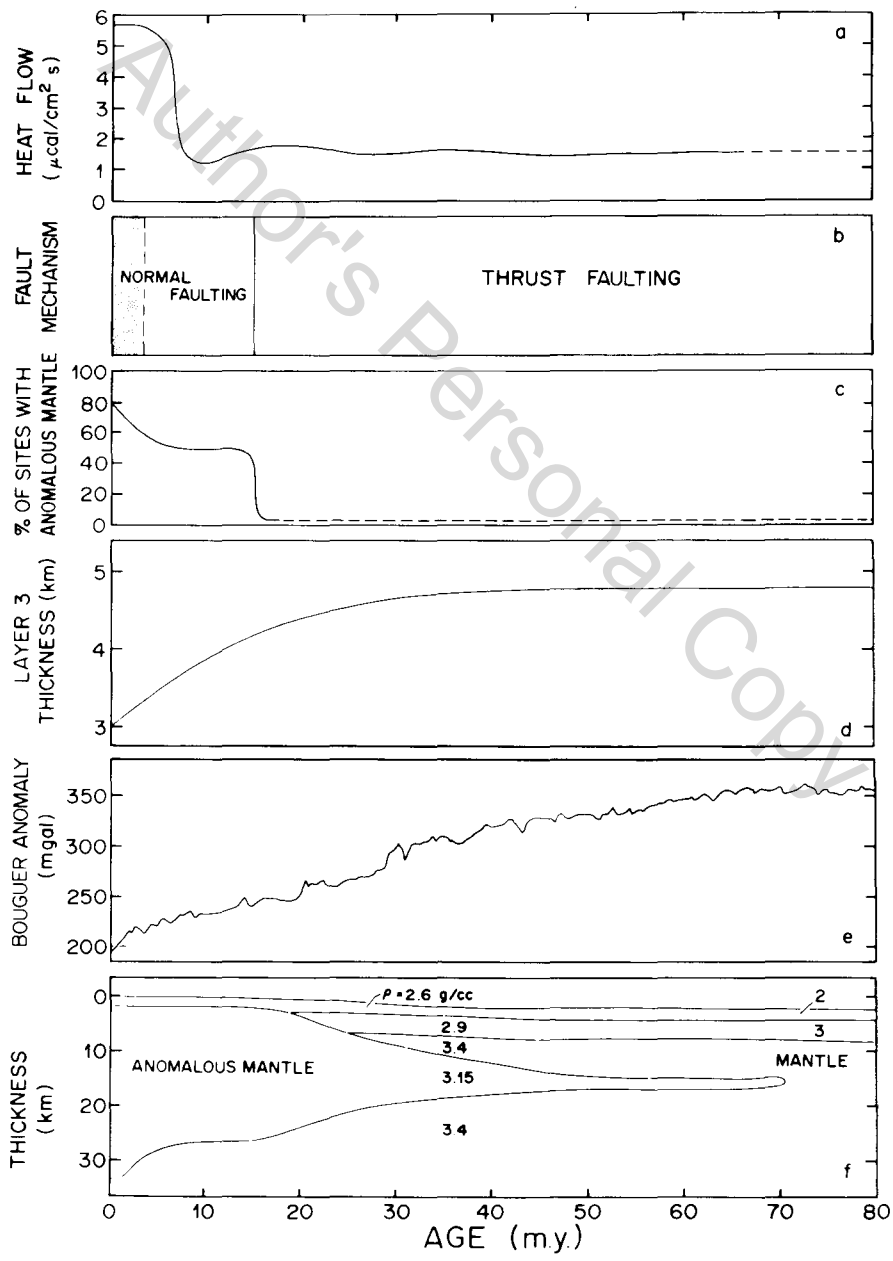

Fig. 22. Geophysical relations at the ridge as a function of sea floor age. The heat flow curve in (*a*) represents the 75% line of *Lee and Uyeda* [1965] for the Atlantic. Fault mechanisms in (*b*) are from *Sykes and Sbar* [1973]; the zone of high seismicity associated with the median valley is indicated by shading. The Bouguer anomaly (*e*) and its interpretation (*f*) are from *Talwani et al.* [1965] for the mid-Atlantic ridge.

petrologic relations in the ophiolites, such support must be embraced with caution. There remains little doubt that the ophiolites derive from the oceanic crust; nonetheless, considerable uncertainty remains concerning the provenance of the ophiolites within the ocean basins themselves. The presence of andesitic basalts and continental clastics in the upper levels of a number of the ophiolites suggests a back-arc basin origin. Alternatively, formation in leaky transform fault zones might explain the presence in many of the ophiolites of an anomalously thin layer 3 and of sheeted dikes perpendicular to the trend of the ridge crests at which they are thought to have been formed. The least restricted, and to us the most attractive, provenance suggested is that the ophiolites are segments of immature ridge crest obducted onto the continental margin during closure of an ocean basin. Such an origin is consistent with the observed youth of the ophiolites at the time of emplacement, the observation that many have metamorphic aureoles at their base, and, again, that most are anomalously thin. Whatever their exact provenance, the ophiolites are not segments of normal oceanic crust. The best that can reasonably be expected is that they are genetically related and petrologically analogous.

In order to consider the mode of origin of the oceanic crust, it is necessary to examine its petrologic structure in light of geophysical relations observed at the mid-ocean ridge (Figure 22). Several authors [*Cann,* 1970; *Greenbaum,* 1972] have suggested that the oceanic crust is formed and essentially completed in a narrow complex of magma chambers, dike swarms, and extrusives immediately underlying the median valley and its associated zone of high heat flow (Figure 22*a* [*Lee and Uyeda,* 1965]). Although crust undoubtedly forms under the median valley, many geophysical phenomena associated with the ridge crest persist far beyond. (1) Most seismicity in the vicinity of the median valley occurs as normal faulting [*Isacks et al.,* 1968], but the seismicity of this mechanism actually continues to approximately 15 m.y., beyond which thrust mechanisms predominate (Figure 22*b* [*Sykes and Sbar,* 1973]). (2) Anomalous mantle velocities are common to 15 m.y. (Figure 22*c*). (3) Layer 3 continues to increase in thickness and volume for 40 m.y. (Figure 22*d*). (4) A strong Bouguer gravity anomaly associated with the presence of the anomalous mantle (masked below the normal mantle beyond 15 m.y.) persists to 70 m.y. (Figures 22*e* and 22*f* [*Talwani et al.,* 1965]).

From these observations it is clear that the formation of oceanic crust is not confined to a narrow vertical zone underlying the ridge median valley. We propose instead that layer 2 and the upper levels of layer 3 form largely under the median valley and that the lower levels of layer 3 thicken under the ridge flanks by offridge intrusion fed from the thinning anomalous mantle in the manner illustrated in Figure 23.

Immediately under the median valley, in a belt coincident with high seismicity and high heat flow, the anomalous mantle rises to shallow levels at many sites, and a liquid tholeiitic fraction continues to the surface via a swarm of continuously spreading tensional dikes to form basaltic extrusives. In primitive stages of crustal development, basaltic extrusives may directly overlie mantle material; in most instances, small turbulent magma chambers, repeatedly invaded from below, serve as staging areas between the mantle and overlying dike swarms to the surface. Seawater, superheated against dike rocks after invasion from above through tension cracks, causes retrograde hydrothermal metamorphism at higher levels.

As this crust moves away from the median valley by sea floor spreading, continued but now intermittent intrusion of magma from the underlying anomalous mantle into the lower levels of layer 3 causes this layer to increase rapidly in

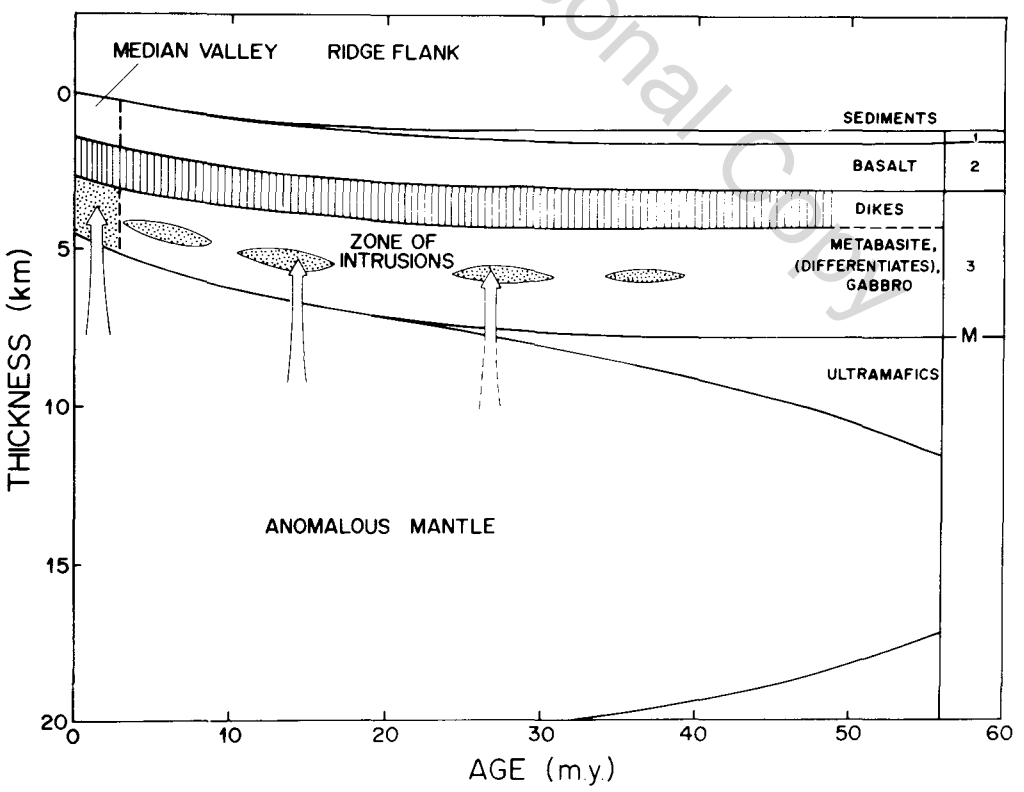

Fig. 23. Generation and evolution of the oceanic crust. The upper levels of the crust are formed largely under the median valley, but layer 3 continues to thicken for nearly 40 m.y. by intermittent offridge intrusion from the anomalous mantle.

thickness. At first, cooling is retarded, and a dense patchwork of cumulate magma chambers, many floored by the anomalous mantle, is maintained. Injection occurs primarily at magmatic levels, and cyclic layering in crystallizing cumulate phases results. Many chambers connect to surface volcanic edifices through late-stage dikes or pipes.

By 15 m.y. the crust is floored, at shallow levels, by a normal mantle composed of cumulate ultramafics and cooled anomalous mantle. Although a change in fault plane solutions at this time suggests that the base of the crust is now locally coupled to mantle convection, gravity anomalies indicate that numerous patches of anomalous mantle still persist at shallow levels in the mantle.

Offridge intrusion, cutting now through the M discontinuity into the lower levels of layer 3, continues to thicken layer 3 at a decelerating pace to 40 m.y., accompanied by minor offridge volcanism and continuous crystallization in the remaining magma chambers, to form massive and cumulate gabbros and, finally, late differentiates. As the crust continues to cool, the final stages of intrusion will be small cross-cutting dikes and apophyses, many with chilled margins, introduced at any level.

Beyond 40 m.y. the lowering of isotherms by continued cooling will introduce retrograde metamorphism to deeper levels. The upper levels of layer 3, becoming chlorite rich, will lower in velocity from 6.8 to approximately 6.5 km/s, as is shown in Figure 3; deeper levels in the gabbro will convert to amphibolite along avenues of water penetration. Should water eventually penetrate to the upper mantle, partial serpentinization would seem inevitable. It should be noted in this regard that the high-velocity basal layer of *Sutton et al.* [1971] has been detected to date only in old crust or in the vicinity of fracture zones.

In the model presented above, we have attempted to explain geophysical observations of the oceanic crust in terms of a petrologic model consistent with information on rocks obtained from dredging. The crustal model adopted was founded in its general form by simple consideration of the rocks reported from oceanic regions, but to obtain information on the relative abundances of these rocks at various levels within the crust, it was necessary to review experimental work bearing on the velocities of compressional and shear waves in oceanic rocks and to compare these velocities with oceanic seismic structure. Within the framework of the model thus obtained, ophiolites represent immature ridge crest that has been obducted at an early stage of crustal evolution onto continental margins, their variability reflecting the complex, almost chaotic, tectonic and intrusive relations at centers of spreading. Thus old crustal segments will rarely be observed on land; their detailed study must await the results of deep-ocean drilling.

Acknowledgments. We are indebted to Tj. H. van Andel, E. Bonatti, R. L. Fisher, J. Hawkins, C. R. B. Lister, and G. Thompson for providing many of the dredge samples used for the experimental studies. Rocks from the Deep-Sea Drilling Project were provided through the assistance of the National Science Foundation. H. Williams gave many helpful suggestions for collecting samples from the Newfoundland ophiolites. In addition, we wish to thank R. McConaghy, M. Mulcahey, P. Lage, G. H. Shaw, R. Ramananantoandro, K. V. Campbell, D. Fountain, R. Carlson, M. Brown, P. Hoddinott, M. Stroh, and J. L. Vance for providing valuable technical support over the past five years for experimental and, in several instances, field phases of this study. Financial support was provided by the Office of Naval Research (contract N-00014-67-A-0103-0014), the National Science Foundation (grant GA-36138), and the Geological Society of America (grant 1680-73).

REFERENCES

Alexandrov, K. S., and T. V. Ryzhova, Elastic properties of rock-forming minerals, 3, Feldspars, *Bull. Acad. Sci. USSR, Geophys. Ser.*, Engl. Transl., no. 2, 129–131, 1962.

Allemann, F., and T. Peters, The ophiolite-radiolarite belt of the North-Oman Mountains, *Eclogae. Geol. Helv., 65*, 657–697, 1972.

Aumento, F., Magmatic evolution on the mid-Atlantic ridge, *Earth Planet. Sci. Lett., 2*, 225–230, 1967.

Aumento, F., The mid-Atlantic ridge near 45°N, 2, Basalts from the area of Confederation Peak, *Can. J. Earth Sci., 5*, 1–21, 1968.

Aumento, F., Diorites from the mid-Atlantic ridge at 45°N, *Science, 165*, 1112–1113, 1969.

Aumento, F., and B. D. Loncarevic, The mid-Atlantic ridge near 45°N, 3, Bald Mountain, *Can. J. Earth Sci., 6*, 11–23, 1969.

Aumento, F., and H. Loubat, The mid-Atlantic ridge near 45°N, 16, Serpentinized ultramafic intrusions, *Can. J. Earth Sci., 8*, 631–663, 1971.

Avias, J., Overthrust structure of the main ultrabasic New Caledonian massives, *Tectonophysics, 4*, 531–541, 1967.

Bailey, E. H., M. C. Blake, Jr., and D. L. Jones, On-land Mesozoic oceanic crust in California coast ranges, *U.S. Geol. Surv. Prof. Pap., 700-C*, C70–C81, 1970.

Barrett, D. L., and F. Aumento, The mid-Atlantic ridge near 45°N, 11, Seismic velocity, density and layering of the crust, *Can. J. Earth Sci., 70*, 1117–1124, 1970.

Bear, L. M., The geology and mineral resources of the Akaki-Lythrodondhe area, *Mem. Geol. Surv. Dep. Cyprus, 3*, 1–122, 1960.

Birch, F., The velocity of compressional waves in rocks to 10 kbar, 1, *J. Geophys. Res., 65*, 1083–1102, 1960.

Birch, F., The velocity of compressional waves in rocks to 10 kbar, 2, *J. Geophys. Res., 66*, 2199–2224, 1961.

Bogdanov, Y. A., and V. V. Ploshko, Magmatic and metamorphic rocks of the Romanche trench, *Dokl. Akad. Nauk. SSSR, 177*, 909–912, 1967.

Bonatti, E., Ultramafic rocks from the mid-Atlantic ridge, *Nature, 219*, 363–364, 1968.

Bonatti, E., J. Honnorez, and G. Ferrara, Equatorial mid-Atlantic ridge: Petrologic and Sr isotopic evidence for an alpine type rock assemblage, *Earth Planet. Sci. Lett., 9*, 247–256, 1970.

Bosshard, E., and D. J. MacFarlane, Crustal structure of the western Canary Islands from seismic refraction and gravity data, *J. Geophys. Res., 75*, 4901–4918, 1970.

Bottinga, Y., Thermal aspects of sea-floor spreading, and the nature of the suboceanic lithosphere, *Tectonophysics, 21*, 15–38, 1974.

Bottinga, Y., and C. J. Allegre, Thermal aspects of sea-floor spreading and the nature of the oceanic crust, *Tectonophysics, 18*, 1–17, 1973.

Bowin, C. O., A. J. Nalwalk, and J. B. Hersey, Serpentinized peridotite from the north wall of the Puerto Rico trench, *Geol. Soc. Amer. Bull., 77*, 257–270, 1966.

Brace, W. F., Resistivity of saturated crustal rocks to 40 km based on laboratory studies, in *The Structure and Physical Properties of the Earth's Crust, Geophys. Monogr. Ser.*, vol. 14, edited by J. G. Hancock, pp. 243–256, AGU, Washington, D. C., 1971.

Brunn, J. H., Contribution à l'étude géologique du Pinde septentrional et d'une partie de la Macedonie occidentale, *Ann. Geol. Pays Hellen., 7*, 1–358, 1956.

Bunce, E. T., and D. A. Fahlquist, Geophysical investigation of the Puerto Rico trench and outer ridge, *J. Geophys. Res., 67*, 3955–3972, 1962.

Bunce, E. T., D. A. Fahlquist, and J. W. Clough, Seismic refraction and reflection measurements—Puerto Rico outer ridge, *J. Geophys. Res., 74*, 3082–3094, 1969.

Cann, J. R., Geological processes at mid-ocean ridge crests, *Geophys. J. Roy. Astron. Soc., 15*, 331–341, 1968.

Cann, J. R., Spilites from the Carlsberg ridge, Indian Ocean, *J. Petrology, 10*, 1–19, 1969.

Cann, J. R., New model for the structure of the ocean crust, *Nature, 226*, 928–930, 1970.

Cann, J. R., and B. M. Funnell, Palmer ridge: A section through the upper part of the ocean crust, *Nature, 213*, 661–664, 1967.

Cann, J. R., and F. J. Vine, An area on the crest of the Carlsberg ridge: Petrology and magnetic survey, *Phil. Trans. Roy. Soc. London, 259*, 198–217, 1966.

Carmichael, D., G. Carpenter, A. Hubbard, K. McCamy, and W. McDonald, A recording ocean bottom seismograph, *J. Geophys. Res., 78*, 8748–8750, 1973.

Chernysheva, V. I., and P. L. Bezrukov, Serpentinite from the crest of the Indo-Arabian ridge, *Dokl. Akad. Nauk SSSR, 166,* 207–210, 1966.

Christensen, N. I., Compressional wave velocities in metamorphic rocks at pressures to 10 kbar, *J. Geophys. Res., 70,* 6147–6164, 1965.

Christensen, N. I., Shear wave velocities in metamorphic rocks at pressures to 10 kbar, *J. Geophys. Res., 71,* 3549–3556, 1966*a*.

Christensen, N. I., Elasticity of ultrabasic rocks, *J. Geophys. Res., 71,* 5921–5931, 1966*b*.

Christensen, N. I., Compressional wave velocities in basic rocks, *Pac. Sci., 22,* 41–44, 1968.

Christensen, N. I., Composition and evolution of the oceanic crust, *Mar. Geol., 8,* 139–154, 1970*a*.

Christensen, N. I., Possible greenschist facies metamorphism of the oceanic crust, *Geol. Soc. Amer. Bull., 81,* 905–908, 1970*b*.

Christensen, N. I., Compressional wave velocities in basalts from the Juan de Fuca ridge, *J. Geophys. Res., 75,* 2773–2775, 1970*c*.

Christensen, N. I., The abundance of serpentinites in the oceanic crust, *J. Geol., 80,* 709–719, 1972*a*.

Christensen, N. I., Seismic anisotropy in the lower oceanic crust, *Nature, 237,* 450–451, 1972*b*.

Christensen, N. I., Compressional and shear wave velocities at pressures to 10 kilobars for basalts from the East Pacific rise, *Geophys. J. Roy. Astron. Soc., 28,* 425–429, 1972*c*.

Christensen, N. I., and R. S. Crosson, Seismic anisotropy in the upper mantle, *Tectonophysics, 6,* 93–107, 1968.

Christensen, N. I., and M. H. Salisbury, Sea floor spreading, progressive alteration of layer 2 basalts, and associated changes in seismic velocities, *Earth Planet. Sci. Lett., 15,* 367–375, 1972.

Christensen, N. I., and M. H. Salisbury, Velocities, elastic moduli and weathering-age relations for Pacific layer 2 basalts, *Earth Planet. Sci. Lett., 19,* 461–470, 1973.

Christensen, N. I., and G. H. Shaw, Elasticity of mafic rocks from the mid-Atlantic ridge, *Geophys. J. Roy. Astron. Soc., 20,* 271–284, 1970.

Church, W. R., and R. K. Stevens, Early Paleozoic ophiolite complexes of the Newfoundland Appalachians as mantle–oceanic crust sequences, *J. Geophys. Res., 76,* 1460–1466, 1971.

Cox, C. S., The electrical conductivity of the oceanic lithosphere, in *The Structure and Physical Properties of the Earth's Crust, Geophys. Monogr. Ser.,* vol. 14, edited by J. G. Hancock, pp. 227–233, AGU, Washington, D. C., 1971.

Davies, H. L., Peridotite-gabbro-basalt complex in eastern Papua: An overthrust plate of oceanic mantle and crust, *Bull. Bur. Mineral Resour. Geol. Geophys. Aust., 128,* 1–47, 1971.

Deffeyes, K. S., The axial valley; a steady-state feature of terrain, in *The Megatectonics of Continents and Oceans,* edited by C. H. Johnson and R. C. Smith, pp. 194–222, Rutgers University Press, Brunswick, N. J., 1970.

Den, N., W. J. Ludwig, S. Murauchi, J. I. Ewing, H. Hotta, N. T. Edgar, T. Yoshii, T. Asanuma, K. Hagiwara, T. Sato, and S. Ando, Seismic refraction measurements in the northwest Pacific basin, *J. Geophys. Res., 74,* 1421–1434, 1969.

Den, N., W. J. Ludwig, S. Murauchi, M. Ewing, H. Hotta, T. Asanuma, T. Yoshii, A. Kubotera, and K. Hagiwara, Sediments and structure of the Eauripik–New Guinea rise, *J. Geophys. Res., 76,* 4711–4723, 1971.

Dengo, G., Tectonic-igneous sequence in Costa Rica, in *Petrologic Studies (Buddington Volume),* edited by A. E. J. Engel, H. L. James, and B. F. Leonard, pp. 133–161, Geological Society of America, Boulder, Colo., 1962.

Dewey, J. F., and J. M. Bird, Origin and emplacement of the ophiolite suite: Appalachian ophiolites in Newfoundland, *J. Geophys. Res., 76,* 3179–3206, 1971.

Dietz, R. S., Alpine serpentines as oceanic rind fragments, *Geol. Soc. Amer. Bull., 74,* 947–752, 1963.

Dortman, N. B., and M. Sh. Magid, New data on velocity of elastic waves in crystalline rocks as a function of moisture, *Int. Geol. Rev., 11,* 517–523, 1969.

Elder, J. W., Physical processes in geothermal areas, in *Terrestrial Heat Flow, Geophys. Monogr. Ser.,* vol. 8, edited by W. H. K. Lee, pp. 211–239, AGU, Washington, D. C., 1965.

Engel, A. E. J., and C. G. Engel, Composition of basalt from the mid-Atlantic ridge, *Science, 144,* 1330–1333, 1964.

Engel, A. E. J., C. G. Engel, and R. G. Havens, Chemical characteristics of oceanic basalts and the upper mantle, *Geol. Soc. Amer. Bull., 76,* 719–734, 1965.

Engel, C. G., and R. L. Fisher, Lherzolite, anorthosite, gabbro and basalt dredged from the mid-Indian Ocean ridge, *Science, 166,* 1136–1141, 1969.

Ewing, J. I., and M. Ewing, Seismic refraction measurements in the Atlantic Ocean basins, in the Mediterranean Sea, on the mid-Atlantic ridge, and in the Norwegian Sea, *Geol. Soc. Amer. Bull., 70,* 291–318, 1959.

Ewing, J. I., and M. Ewing, Sediment distribution on the mid-ocean ridges with respect to spreading of the sea-floor, *Science, 156,* 1590–1593, 1967.

Ewing, J. I., and R. Houtz, Mantle reflections in air gun–sonobuoy profiles, *J. Geophys. Res., 74,* 6706–6709, 1969.

Ewing, J. I., W. J. Ludwig, M. Ewing, and S. L. Eittreim, Structure of the Scotia Sea and Falkland plateau, *J. Geophys. Res., 76,* 7118–7137, 1971.

Ewing, M., A. P. Crary, and H. M. Rutherford, Geophysical investigations in the emerged and submerged Atlantic coastal plain, 1, Methods and results, *Geol. Soc. Amer. Bull., 48,* 753–802, 1937.

Ewing, M., G. P. Woollard, and A. C. Vine, Geophysical investigations in the emerged and submerged Atlantic coastal plain, 3, Barnegat Bay, New Jersey, section, *Geol. Soc. Amer. Bull., 50,* 257–296, 1939.

Ewing, M., L. V. Hawkins, and W. J. Ludwig, Crustal structure of the Coral Sea, *J. Geophys. Res., 75,* 1953–1962, 1970.

Fenwick, D. K. B., M. J. Keen, C. Keen, and A. Lambert, Geophysical studies of the continental margin northeast of Newfoundland, *Can. J. Earth Sci., 5,* 483–500, 1968.

Fisher, R. L., and C. G. Engel, Ultramafic and basaltic rocks dredged from the nearshore flank of the Tonga trench, *Geol. Soc. Amer. Bull., 80,* 1373–1378, 1969.

Fox, P. J., E. Schreiber, and B. C. Heezen, The geology of the Caribbean crust: Tertiary rocks from the Aves ridge, *Tectonophysics, 12,* 89–109, 1971.

Fox, P. J., E. Schreiber, and J. J. Peterson, The geology of the oceanic crust: Compressional wave velocities of oceanic rocks, *J. Geophys. Res., 78,* 5155–5172, 1973.

Francis, T. G., and I. T. Porter, Median valley seismology: The mid-Atlantic ridge near 45°N, *Geophys. J. Roy. Astron. Soc., 34,* 279–311, 1973.

Francis, T. G., and R. W. Raitt, Seismic refraction measurements in the southern Indian Ocean, *J. Geophys. Res., 72,* 3015–3041, 1967.

Francis, T. G., and G. G. Shor, Jr., Seismic refraction measurements in the northwest Indian Ocean, *J. Geophys. Res., 71,* 427–449, 1966.

Furumoto, A. S., G. P. Woollard, J. F. Campbell, and D. M. Hussong, Variation in the thickness of the crust in the Hawaiian archipelago, in *The Crust and Upper Mantle of the Pacific Area, Geophys. Monogr. Ser.,* vol. 12, edited by L. Knopoff, C. L. Drake, and P. J. Hart, pp. 94–111, AGU, Washington, D. C., 1968.

Furumoto, A. S., J. F. Campbell, and D. M. Hussong, Seismic refraction surveys along the Hawaiian ridge, Kauai to Midway, *Bull. Seismol. Soc. Amer., 61,* 147–166, 1971.

Gansser, A., *The Geology of the Himalayas,* pp. 123–128, Interscience, New York, 1964.

Gass, I. G., Is the Troodos massif of Cyprus a fragment of Mesozoic ocean floor?, *Nature, 220,* 39–42, 1968.

Gass, I. G., and D. Masson-Smith, The geology and gravity anomalies of the Troodos massif, Cyprus, *Phil. Trans. Roy. Soc. London, Ser. A, 255,* 417–467, 1963.

Gass, I. G., and J. D. Smewing, Intrusion, extrusion and metamorphism at constructive margins: Evidence from the Troodos massif, Cyprus, *Nature, 242,* 26–29, 1973.

Goslin, J., P. Beauzart, J. Francheteau, and X. Le Pichon, Thickening of the oceanic layer in the Pacific Ocean, *Mar. Geophys. Res., 1,* 418–427, 1972.

Greenbaum, D., Magmatic processes at ocean ridges: Evidence from the Troodos massif, Cyprus, *Nature Phys. Sci., 238,* 18–21, 1972.

Gutenberg, B., *Physics of the Earth's Interior,* pp. 28–36, Academic, New York, 1959.

Hart, R. A., Chemical exchange between sea water and deep ocean basalts, *Earth Planet. Sci. Lett., 9,* 269–279, 1970.

Hart, R. A., A model for chemical exchange in the basalt-seawater system of oceanic layer II, *Can. J. Earth Sci., 10,* 799–816, 1973.

Hawkins, J. W., J. G. Sclater, and G. Hornhaus, Petrologic and geophysical characteristics of the Lau basin ridge—A spreading center behind the Tonga arc (abstract), *Geol. Soc. Amer. Abstr. Programs, 2,* 571, 1970.

Hekinian, R., Rocks from the mid-oceanic ridge in the Indian Ocean, *Deep Sea Res., 15,* 195–213, 1968.

Hekinian, R., Chemical and mineralogical differences between abyssal hill basalts and ridge tholeiites in the eastern Pacific Ocean, *Mar. Geol., 11,* 77–91, 1971.

Hekinian, R., and F. Aumento, Rocks from the Gibbs fracture zone and the Minia seamount near 53°N in the Atlantic Ocean, *Mar. Geol., 14,* 47–72, 1973.

Helmberger, D. V., The crust-mantle transition in the Bering Sea, *Bull. Seismol. Soc. Amer., 58,* 179–214, 1968.

Helmberger, D. V., and G. B. Morris, A travel time and amplitude interpretation of a marine refraction profile: Primary waves, *J. Geophys. Res., 74,* 483–494, 1969.

Helmberger, D. V., and G. B. Morris, A travel time and amplitude interpretation of a marine refraction profile: Transformed shear waves, *Bull. Seismol. Soc. Amer., 60,* 593–600, 1970.

Hess, H. H., History of ocean basins, in *Petrologic Studies (Buddington Volume),* edited by A. E. J. Engel, H. L. James, and B. F. Leonard, pp. 599–620, Geological Society of America, Boulder, Colo., 1962.

Hess, H. H., Seismic anisotropy of the uppermost mantle under oceans, *Nature, 203,* 629–631, 1964*a*.

Hess, H. H., The oceanic crust, the upper mantle and the Magaguez serpentinized peridotite, in *A Study of Serpentinite, Publ. 1188,* edited by C. A. Burke, pp. 169–175, National Academy of Sciences–National Research Council, Washington, D. C., 1964*b*.

Hill, M. N., Seismic refraction shooting in an area of the eastern Atlantic, *Phil. Trans. Roy. Soc. London, Ser. A, 244,* 561–596, 1952.

Hill, M. N., Recent geophysical exploration of the ocean floor, *Phys. Chem. Earth, 2,* 129–163, 1957.

Hopson, C. A., and J. M. Mattinson, Ordovician and Late Jurassic ophiolite assemblages in the Pacific Northwest (abstract), *Geol. Soc. Amer. Abstr. Programs, 5,* 57, 1973.

Houtz, R., J. I. Ewing, and P. Buhl, Seismic data from sonobuoy stations in the northern and equatorial Pacific, *J. Geophys. Res., 75,* 5093–5111, 1970.

Hughes, D. S., and J. L. Kelly, Variation of elastic wave velocity with saturation in sandstone, *Geophysics, 17,* 739–752, 1952.

Hussong, D. M., Detailed structural interpretations of the Pacific oceanic crust using ASPER and ocean bottom seismometer methods, Ph.D. thesis, 165 pp., Univ. of Hawaii, Honolulu, 1972.

Hussong, D. M., A. A. Nowroozi, M. E. Odegard, and G. H. Sutton, Crustal structure under an ocean bottom seismometer using explosive sources (abstract), *Eos Trans. AGU, 50,* 644, 1969.

Hyndman, R. D., Seismic velocities of basalts from DSDP leg 26 (abstract), *Eos Trans. AGU, 54,* 1026, 1973.

Ingle, J. C., Jr., D. E. Karig, A. H. Bouma, C. H. Ellis, N. Haile, I. Koizumi, H. Y. Ling, I. MacGregor, C. Moore, H. Ujiie, T. Watanabe, S. M. White, and M. Yasui, Western Pacific floor, *Geotimes, 18,* 22–25, 1973.

Isacks, B., J. Oliver, and L. R. Sykes, Seismology and the new global tectonics, *J. Geophys. Res., 73,* 5855–5899, 1968.

Karig, D. E., Structural framework of the west Philippine basin (abstract), *Geol. Soc. Amer. Abstr. Programs, 4,* 180–181, 1972.

Kay, R., N. J. Hubbard, and P. Gast, Chemical characteristics and origin of oceanic ridge volcanic rocks, *J. Geophys. Res., 75,* 1581–1613, 1970.

Keen, C. E., and D. L. Barrett, A measurement of seismic anisotropy in the Northeast Pacific, *Can. J. Earth Sci., 8,* 1056–1064, 1971.

Keen, C. E., and B. D. Loncarevic, Crustal structure on the eastern seaboard of Canada: Studies on the continental margin, *Can. J. Earth Sci., 3,* 65–76, 1966.

Kundig, E., Geology and ophiolite problems of East-Celebes, *Verh. Kon. Ned. Geol. Mijnbouwk. Genoot., 16,* 210–235, 1956.

Lee, W. H. K., and S. Uyeda, Review of heat flow data, in *Terrestrial Heat Flow, Geophys. Monogr. Ser.,* vol. 8, edited by W. H. K. Lee, pp. 87–190, AGU, Washington, D. C., 1965.

Le Pichon, X., Models and structure of the oceanic crust, *Tectonophysics, 7,* 385–401, 1969.

Le Pichon, X., R. E. Houtz, C. L. Drake, and J. E. Nafe, Crustal structure of the mid-ocean ridges, 1, Seismic refraction measurements, *J. Geophys. Res., 70,* 319–339, 1965.

Lister, C. R. B., On the thermal balance of a mid-ocean ridge, *Geophys. J. Roy. Astron. Soc., 26,* 515–535, 1972.

Lister, C. R. B., and B. T. R. Lewis, An ocean bottom seismometer suitable for arrays (abstract), *Eos Trans. AGU, 55,* 357, 1974.

Ludwig, W. J., J. I. Ewing, M. Ewing, S. Murauchi, N. Den, S. Asano, H. Hotta, M. Hayakawa, T. Asanuma, K. Ichikawa, and I. Ichikawa, Sediments and structure of the Japan trench, *J. Geophys. Res., 71,* 2121–2137, 1966.

Ludwig, W. J., J. E. Nafe, E. S. W. Simpson, and S. Sacks, Seismic refraction measurements on the southeast African continental margin, *J. Geophys. Res., 73,* 3707–3719, 1968.

Ludwig, W. J., S. Murauchi, N. Den, M. Ewing, H. Hotta, R. Houtz, T. Yoshii, T. Asanuma, K. Hagiwara, T. Sato, and S. Ando, Structure of Bowers ridge, Bering Sea, *J. Geophys. Res., 76,* 6350–6375, 1971.

Ludwig, W. J., S. Murauchi, N. Den, P. Buhl, H. Hotta, M. Ewing, T. Asanuma, T. Yoshii, and N. Sakajiri, Structure of east China Sea–west Philippine Sea margin off southern Kyushu, Japan, *J. Geophys. Res., 78,* 2526–2536, 1973.

Matthews, D. H., A. S. Laughton, D. T. Pugh, E. T. W. Jones, J. Sunderland, M. Takin, and M. Bacon, Crustal structure and origin of Peake and Freen deeps, N.E. Atlantic, *Geophys. J. Roy. Astron. Soc., 18,* 517–542, 1969.

Maynard, G. L., G. H. Sutton, and D. M. Hussong, Seismic observations in the Solomon Islands and Darwin rise regions using repetitive sources (abstract), *Eos Trans. AGU, 50,* 206, 1969.

McConnell, R. K., Jr., R. N. Gupta, and J. T. Wilson, Compilation of deep crustal seismic refraction profiles, *Rev. Geophys. Space Phys., 4,* 41–100, 1966.

Melson, W. G., and G. Thompson, Layered basic complex in oceanic crust, Romanche fracture, equatorial Atlantic Ocean, *Science, 168,* 817–820, 1970.

Melson, W. G., and G. Thompson, Petrology of a transform fault zone and adjacent ridge segments, *Phil. Trans. Roy. Soc. London, Ser. A, 268,* 423–441, 1971.

Melson, W. G., and Tj. H. van Andel, Metamorphism in the mid-Atlantic ridge, 22°N. latitude, *Mar. Geol., 4,* 165–186, 1966.

Menard, H. W., Sea-floor spreading, topography and the second layer, *Science, 157,* 923–924, 1967.

Miyashiro, A., The Troodos ophiolite complex was probably formed in an island arc, *Earth Planet. Sci. Lett., 19,* 218–224, 1973.

Miyashiro, A., F. Shido, and M. Ewing, Composition and origin of serpentinites from the mid-Atlantic ridge near 24° and 30° north latitude, *Contrib. Mineral. Petrol., 23,* 117–127, 1969*a*.

Miyashiro, A., F. Shido, and M. Ewing, Diversity and origin of abyssal tholeiite from the mid-Atlantic ridge near 24° and 30° north latitude, *Contrib. Mineral. Petrol., 23,* 38–52, 1969*b*.

Miyashiro, A., F. Shido, and M. Ewing, Crystallization and differentiation in abyssal tholeiites and gabbros from mid-oceanic ridges, *Earth Planet. Sci. Lett., 7,* 361–365, 1970*a*.

Miyashiro, A., F. Shido, and M. Ewing, Petrologic models for the mid-Atlantic ridge, *Deep Sea Res., 17,* 109–123, 1970*b*.

Miyashiro, A., F. Shido, and M. Ewing, Metamorphism in the mid-Atlantic ridge near 24° and 30°N, *Phil. Trans. Roy. Soc. London, Ser. A, 268,* 589–603, 1971.

Moores, E. M., Petrology and structure of the Vourinos ophiolitic complex of northern Greece, *Geol. Soc. Amer. Spec. Pap., 118,* 1–74, 1969.

Moores, E. M., Reexamination of the Vourinos ophiolite, Greece (abstract), *Eos Trans. AGU, 55,* 444, 1974.

Moores, E. M., and E. M. Jackson, Ophiolites and ocean crust, *Nature, 250,* 136–139, 1974.

Moores, E. M., and F. J. Vine, The Troodos massif, Cyprus, and other ophiolites as oceanic crust: Evaluation and implications, *Phil. Trans. Roy. Soc. London, Ser. A, 268,* 443–466, 1971.

Muir, I. D., and C. E. Tilley, Basalts from the northern part of the mid-Atlantic ridge, *J. Petrology, 7,* 193–211, 1966.

Murauchi, S., N. Den, S. Asano, H. Hotta, T. Yoshii, T. Asanuma, K. Hagiwara, K. Ichikawa, T. Sato, W. J. Ludwig, J. I. Ewing, N. T. Edgar, and R. E. Houtz, Crustal structure of the Philippine Sea, *J. Geophys. Res., 73,* 3143–3171, 1968.

Murauchi, S., W. J. Ludwig, N. Den, H. Hotta, T. Asanuma, T. Yoshii, A. Kubotera, and K. Hagiwara, Structure of the Sulu Sea and the Celebes Sea, *J. Geophys. Res., 78,* 3437–3447, 1973.

Nicholls, G. D., A. J. Nalwalk, and E. E. Hays, The nature and composition of rock samples dredged from the mid-Atlantic ridge between 22°N and 52°N, *Mar. Geol., 1,* 333–343, 1964.

Nur, A., and G. Simmons, The effect of saturation on velocity in low porosity rocks, *Earth Planet. Sci. Lett., 7,* 183–193, 1969.

Officer, C. B., J. I. Ewing, J. F. Hennion, D. G. Harkrider, and D. E. Miller, Geophysical investigations in the eastern Caribbean: Summary of 1955 and 1956 cruises, *Phys. Chem. Earth, 3,* 17–109, 1959.

Oxburgh, E. R., and D. L. Turcotte, Mid-ocean ridges and geotherm

distribution during mantle convection, *J. Geophys. Res.*, *73*, 2643–2661, 1968.

Page, B. M., Oceanic crust and mantle fragment in subduction complex near San Luis Obispo, California, *Geol. Soc. Amer. Bull.*, *83*, 957–972, 1972.

Pamić, J., Some petrological features of Bosnian peridotite-gabbro complexes in the Dinaride zone of Yugoslavia, *Tschermaks Mineral. Petrogr. Mitt.*, *15*, 14–42, 1971.

Peterson, J. J., P. J. Fox, and E. Schreiber, Newfoundland ophiolites and the geology of the oceanic layer, *Nature*, *247*, 194–196, 1974.

Phillips, J. D., G. Thompson, R. P. Von Herzen, and V. T. Bowen, Mid-Atlantic ridge near 43°N latitude, *J. Geophys. Res.*, *74*, 3069–3081, 1969.

Ploshko, V. V., and Y. A. Bogdanov, Ultrabasites of the deep-water Romanche trench, *Izv. Akad. Nauk SSSR*, *12*, 82–93, 1968.

Poster, C. K., Ultrasonic velocities in rocks from the Troodos massif, Cyprus, *Nature*, *243*, 2–3, 1973.

Quon, S. H., and E. G. Ehlers, Rocks of the northern part of the mid-Atlantic ridge, *Geol. Soc. Amer. Bull.*, *74*, 1–7, 1963.

Raitt, R. W., The crustal rocks, in *The Sea*, vol. 3, edited by M. N. Hill, pp. 85–102, John Wiley, New York, 1963.

Raitt, R. W., G. G. Shor, Jr., G. B. Morris, and H. K. Kirk, Mantle anisotropy in the Pacific Ocean, *Tectonophysics*, *12*, 173–186, 1971.

Reinhardt, B. M., On the genesis and emplacement of ophiolites in the Oman Mountains geosyncline, *Schweiz. Mineral. Petrogr. Mitt.*, *49*, 1–30, 1969.

Rigo de Righi, M., and A. Cortesina, Gravity tectonics in foothills structure belt of southeast Turkey, *Amer. Ass. Petrol. Geol. Bull.*, *48*, 1911–1937, 1964.

Ryzhova, T. V., Elastic properties of plagioclase, *Bull. Acad. Sci. USSR, Geophys. Ser.*, Engl. Transl., no. 7, 633–635, 1964.

Shido, F., A. Miyashiro, and M. Ewing, Crystallization of abyssal tholeiites, *Contrib. Mineral. Petrol.*, *31*, 251–266, 1971.

Shor, G. G., Jr., Refraction and reflection techniques and procedure, in *The Sea*, vol. 3, edited by M. N. Hill, pp. 20–38, John Wiley, New York, 1963.

Shor, G. G., Jr., P. Dehlinger, H. K. Kirk, and W. S. French, Seismic refraction studies off Oregon and northern California, *J. Geophys. Res.*, *73*, 2175–2194, 1968.

Shor, G. G., Jr., H. W. Menard, and R. W. Raitt, Structure of the Pacific basin, in *The Sea*, vol. 4, edited by A. E. Maxwell, pp. 3–27, John Wiley, New York, 1971*a*.

Shor, G. G., Jr., H. K. Kirk, and H. W. Menard, Crustal structure of the Melanesian area, *J. Geophys. Res.*, *76*, 2562–2586, 1971*b*.

Simmons, G., The velocity of shear waves in rocks to 10 kbar, 1, *J. Geophys. Res.*, *69*, 1123–1130, 1964.

Smith, C. H., Bay of Islands igneous complex, western Newfoundland, *Geol. Surv. Can. Mem.*, *290*, 1–132, 1958.

Steinmann, A., Die ophiolitischen Zonen in den mediterranen Kettengebirgen, *Int. Geol. Congr. 14th*, *2*, 637–667, 1926.

Sutton, G. H., G. L. Maynard, and D. M. Hussong, Marine crustal seismic refraction studies using repetitive sources and sonobuoys (abstract), in *Program of Annual Meeting*, Seismological Society of America, Oakland, Calif., 1969.

Sutton, G. H., G. L. Maynard, and D. M. Hussong, Widespread occurrence of a high-velocity basal layer in the Pacific crust found with repetitive sources and sonobuoys, in *The Structure and Physical Properties of the Earth's Crust, Geophys. Monogr. Ser.*, vol. 14, edited by J. G. Heacock, pp. 193–209, AGU, Washington, D. C., 1971.

Switzer, A., A. Melson, and G. Thompson, Garnet from the mid-Atlantic ridge near 43°N latitude, *Geol. Soc. Amer. Bull.*, *81*, 895–898, 1970.

Sykes, L. R., and M. L. Sbar, Intraplate earthquakes, lithospheric stresses and the driving mechanism of plate tectonics, *Nature*, *245*, 298–302, 1973.

Talwani, M., X. Le Pichon, and M. Ewing, Crustal structure of the mid-oceanic ridges, 2, Computed model from gravity and seismic refraction data, *J. Geophys. Res.*, *70*, 341–352, 1965.

Talwani, M., C. C. Windisch, and M. G. Langseth, Jr., Reykjanes ridge crest: A detailed geophysical study, *J. Geophys. Res.*, *76*, 473–517, 1971.

Thayer, T. P., The Canyon Mountain complex, Oregon, and the Alpine mafic magma stem, *U.S. Geol. Surv. Prof. Pap.*, *475C*, C82–C85, 1963.

Thompson, G., Trace-element distributions in fractionated oceanic rocks, 2, Gabbros and related rocks, *Chem. Geol.*, *12*, 99–111, 1973.

Thompson, G., and W. G. Melson, The petrology of oceanic crust across fracture zones in the Atlantic Ocean: Evidence of a new kind of sea-floor spreading, *J. Geol.*, *80*, 526–538, 1972.

Upadhyay, H. D., J. F. Dewey, and E. R. W. Neale, The Betts cove ophiolite complex, Newfoundland: Appalachian oceanic crust and mantle, *Proc. Geol. Ass. Can.*, *24*, 27–34, 1971.

van Andel, Tj. H., J. D. Phillips, and R. P. Von Herzen, Rifting origin for the Vema fracture in the North Atlantic, *Earth Planet. Sci. Lett.*, *5*, 296–300, 1969.

Varne, R., and M. J. Rubenach, Geology of Macquarie Island and its relationship to oceanic crust, in *Antarctic Oceanology II: The Australian–New Zealand Sector, Antarctic Res. Ser.*, vol. 19, edited by D. E. Hayes, pp. 251–266, AGU, Washington, D. C., 1972.

Varne, R., R. D. Gee, and P. G. J. Quilty, Macquarie Island and the cause of oceanic linear magnetic anomalies, *Science*, *166*, 230–232, 1969.

Vuagnat, M., Remarques sur la trilogie serpentinites-gabbros-diabases dans le basin de la Méditerranée occidentale, *Geol. Rundsch.*, *53*, 336–358, 1963.

Vine, F. T., and H. H. Hess, Sea floor spreading, in *The Sea*, vol. 4, edited by A. E. Maxwell, pp. 587–622, John Wiley, New York, 1971.

Vine, F. J., C. K. Poster, and I. G. Gass, Aeromagnetic survey of the Troodos igneous massif, Cyprus, *Nature Phys. Sci.*, *244*, 34–38, 1973.

Wager, L. R., and W. A. Deer, Geological investigations in east Greenland, 3, The petrology of the Skaergaard intrusion, Kangerdluzssaug, east Greenland, *Medd. Groenland*, *105*, 1–353, 1939.

Wenner, D. B., and H. P. Taylor, Jr., Oxygen and hydrogen isotope studies of the serpentinization of ultramafic rocks in oceanic environments and continental ophiolite complexes, *Amer. J. Sci.*, *273*, 207–239, 1973.

Whitmarsh, R. B., Seismic anisotropy of the uppermost mantle absent beneath the east flank of the Reykjanes ridge, *Bull. Seismol. Soc. Amer.*, *61*, 1351–1368, 1971.

Williams, H., Mafic-ultramafic complexes in western Newfoundland Appalachians and the evidence for transportation: A review and interim report, *Proc. Geol. Ass. Can.*, *24*, 9–25, 1971.

Williams, H., and J. Malpas, Sheeted dikes and brecciated dike rocks within transported igneous complexes, Bay of Islands, western Newfoundland, *Can. J. Earth Sci.*, *9*, 1216–1229, 1972.

Wyllie, M. R. J., A. R. Gregory, and G. H. F. Gardner, An experimental investigation of factors affecting elastic wave velocities in porous media, *Geophysics*, *23*, 459–493, 1958.

Yoshii, T., W. J. Ludwig, N. Den, S. Murauchi, M. Ewing, H. Hotta, P. Buhl, T. Asanuma, and N. Sakajiri, Structure of southwest Japan margin of Shikoku, *J. Geophys. Res.*, *78*, 2517–2525, 1973.

(Received June 18, 1974;
accepted September 10, 1974.)